

Transforming the Petroleum Industry through Catalytic Oxidation Reactions vis-à-vis Preceramic Polymer Catalyst Supports

Williams Kweku Darkwah,* Alfred Bekoe Appiagyei, and Joshua B. Puplampu



Cite This: *ACS Omega* 2023, 8, 34215–34234



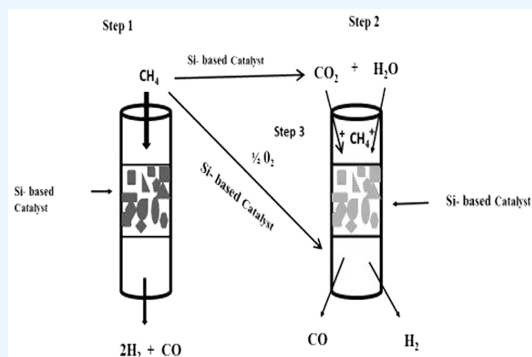
Read Online

ACCESS |

Metrics & More

Article Recommendations

ABSTRACT: Preceramic polymers, for instance, are used in a variety of chemical processing industries and applications. In this contribution, we report on the catalytic oxidation reactions generated using preceramic polymer catalyst supports. Also, we report the full knowledge of the use of the remarkable catalytic oxidation, and the excellent structures of these preceramic polymer catalyst supports are revealed. This finding, on the other hand, focuses on the functionality and efficacy of future applications of catalytic oxidation of preceramic polymer nanocrystals for energy and environmental treatment. The aim is to design future implementations that can address potential environmental impacts associated with fuel production, particularly in downstream petroleum industry processes. As a result, these materials are being considered as viable candidates for environmentally friendly applications such as refined fuel production and related environmental treatment.



INTRODUCTION

Compared to diesel engines, heavy-duty engines that run on natural gas or biogas emit fewer pollutants like soot and NO_x but release more hydrocarbon gases like methane and ethane. Because of methane's considerable greenhouse effect, it is vital to reduce and manage methane emissions from natural gas cars. Several catalysts (basically single atom catalysts, or SACs) have been developed for the wide-ranging oxidation of methane in the exhaust stream in response to a variety of permitted methane emission criteria, which is a promising strategy that allows for high combustion efficiency.^{2–4} Most commercial catalysts, including palladium, nickel, and platinum, are supported by nanoscale preceramic polymers, monolithic honeycomb, and other catalyst support materials that meet the performance requirements of the petroleum industries.

Silicon carbide (SiC), a preceramic polymer, has quite a long history of increasing in importance as a catalyst support material,⁵ corresponding to its progress in a variety of optoelectronic device elements, lightweight or high strength structures, biomedical materials, and high-temperature semiconductor devices. To achieve successful catalysis, a low surface area of SiC-type was synthesized utilizing a block copolymer as a precursor and a preceramic polymer template. This was done to overcome the limits of commercially available SiC.^{6,7}

The process of increasing the rate of a reaction in the presence of a catalyst is known as catalysis. The most common media for catalytic processes includes gas phase, pure organic liquid phases, and aqueous solutions. Moreover, catalysts are

often highly effective in regulating organic wastewater, solar energy utilization, and environmental treatment applications, particularly in catalytic reduction involving photons and environmental treatment applications. The application of catalysis in the petroleum industry is based on a fundamental principle, and the catalytic reaction can be used to produce energy or eliminate pollutants. These reactions often involve converting synthesis gas into usable hydrocarbons, which are used in industrial processes as an alternative fuel to crude oil. It involves reforming coal, natural gas, or biomass using steam and oxygen to produce a mixture of predominantly CO, CH₄, CH₃OH, and H₂.² In general, the advantages and disadvantages of catalytic oxidation reactions could be considered. Catalytic oxidation is recognized as one of the most effective cleaning procedures due to its ability to break down tough organic particles as well as its multiple benefits including low energy consumption, no additional pollution, and user-friendliness.

A catalyst can aid in increasing energy recovery. The heat emitted by burning in automotive exhaust catalysts is dispersed into the air, while the heat generated by oxidation can be used in a chemical plant to reduce pollution.⁸ Catalytic heaters,

Received: November 25, 2022

Accepted: April 21, 2023

Published: September 12, 2023



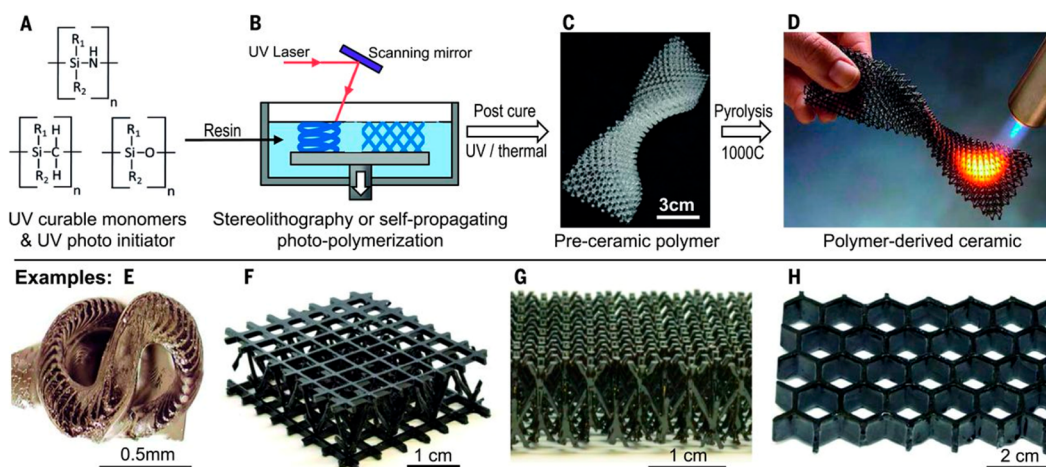


Figure 1. Additive manufacturing of polymer-derived ceramics. (A) UV-curable preceramic monomers are mixed with photoinitiator. (B) The resin is exposed with UV light in an SLA 3D printer or through a patterned mask. (C) A preceramic polymer part is obtained. (D) Pyrolysis converts the polymer into a ceramic. Examples: (E) SLA 3D printed corkscrew. (F and G) SPPW formed microlattices. (H) Honeycomb. Adapted with permission from ref 208. Copyright from Science, 2016.

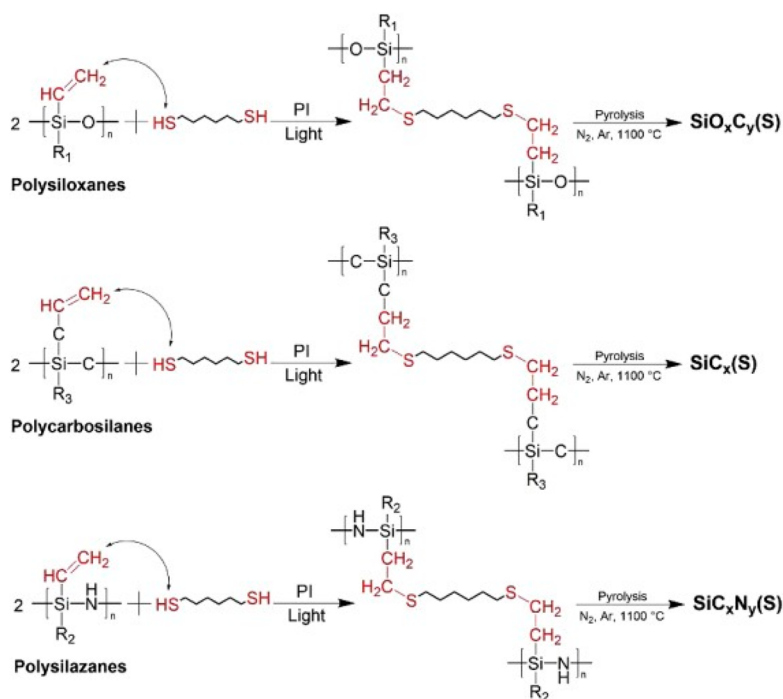


Figure 2. Structural summary for synthesis of preceramic polymers, polysiloxanes, polycarbosilanes, and polysilazanes, to SiC, Si_xC_y, and SiO_xC_y, vis-à-vis pyrolysis.

which typically consist of catalysts supported by a fibrous pad, generate heat.^{1,9}

There are several disadvantages to using catalytic combustors. Catalysts are usually expensive and have a limited lifespan. Adsorption can poison the catalyst at low temperatures where oxidation is not an issue. Moreover, the catalysts must function at high temperatures, which may require the use of metal or sintering support. In extreme situations, it may even melt, causing molten ceramic to spill out of the reactor: in such cases, the properties of the fuel under consideration are often used to determine whether to shift off the fuel stream.

This paper focuses on the potential of catalytic oxidation using preceramic polymer nanocrystals for energy and

environmental treatment, to design future implementations to address environmental issues associated with fuel production, particularly in downstream petroleum industry processes.

We will examine the relationship between oxidative processes, nanoscale synthesis of Si preceramic polymer-based catalysts, and catalytic structures as an example. This information is particularly useful in the creation of better catalytic oxidation–reduction systems. The ramifications of our increased understanding for current catalytic oxidation reactions to generate alternative fuels to fossil fuels will be another focus of our research. As a result, these materials are being considered as potential options for environmentally

friendly applications like refined fuel manufacturing and wastewater treatment.

■ SI-DERIVED PRECERAMIC POLYMERS

Preceramic polymers, for instance, find applications in various chemical processing industries and applications. Clean fuel based on oxidation is crucial in sectors such as chemical recovery and purification. Silica, conventional alumina, silica–alumina, and preceramic polymer-based materials such as silicon carbide (SiC) are used as catalyst supports in chemical and petroleum processing reactions such as hydrocracking, direct and partial oxidation, reforming, and polymerization.

Silicon-derived polymers with nitrogen, carbon, and boron have been postulated as precursors for nonoxide ceramics such as SiC, SiCN, and SiBCN.^{186,191,192} Polysiloxanes and polycarbosilanes are two types of preceramic polymers that can be easily manufactured using a variety of techniques before being cross-linked with heat or UV radiation to form an infusible solid (see the preparation process in Figure 1). Pyrolysis of consolidated preceramic polymers at high temperatures produces thick ceramic phases (Figures 1 and 2). High-temperature applications for these materials include structural composites,¹⁹⁰ electrical devices,¹⁸⁸ and catalytic chemical reactions.^{189,190}

One of the most appealing aspects of using polymeric precursors is the simplicity of synthesis at low processing temperatures. Because preceramic polymers with moderate molecular weights are easily soluble in organic solvents such as cyclohexane, THF, and xylene, they can be easily spun, dip-coated, or spray-coated onto metal, ceramic, or graphite surfaces to focus on improving anticorrosion, catalytic oxidation, and antioxidation properties. After cross-linking and heat treatment, preceramic polymers become amorphous ceramic at extreme temperatures from 600 to 1100 °C (Figure 1) and crystalline ceramic at temperatures over 1200 °C. The polymer precursors used have a significant impact on the chemical composition and microstructure of the final ceramic.

Direct infiltration of low viscosity allylhydrido polycarbosilane into a randomly packed silica colloidal sphere template with a diameter of 20 to 30 nm, like the process used to generate microporous SiC, was proven in a report on the fabrication of mesoporous SiC utilizing a preceramic polymer. The disordered mesoporous SiC amorphous foam-like structure has a huge surface area and a total pore volume of 0.81 cm³ g⁻¹.¹⁸⁷ Preceramic mesoporous SiC exhibited no long-range order of porosity because the silica nanospheres could not be precipitated into a closed-packed structure due to substantial electrostatic interactions between spheres.

Preceramic polymers are a form of polymer that can be turned into ceramic when heated to temperatures exceeding 800 °C.²⁰⁴ One approach for preparing preceramic polymers is microcomponent processing employing UV/electron beam lithography.^{205,206} In the photolithography process, it is a type of lithography that uses UV light or an electron beam as an illumination source to transfer a pattern into a substrate (see Figure 1). However, there has been minimal research into using photolithography to process preceramic polymers, with most research focusing on microfluidic processing or soft lithography and polymer-derived ceramics (PDCs).^{205,207} Preceramic polymers are a form of polymer that can be turned into ceramics by heating them above 800 °C.²⁰⁴

■ POLYSILOXANES

These polymers have a wide range of uses, particularly in high-tech industries. In the aerospace industry, where semiconductor materials are used to create silicon wafers, these materials are extremely valuable. This polymer family has several intriguing features, and as technology advances, the polysiloxane industry will likely expand even more, allowing for new applications like lithography.^{20,209} The synthesis, characterization, and use of ceramic materials made by controlled pyrolysis of preceramic polymers including diverse fillers have all been proven to be crucial for crystallization behavior.^{205,210,211} One of these processes for generation is pyrolysis. Pyrolysis is the process of crushing nanoalumina particles with polysiloxane samples at 1500 °C in an inert argon environment (Figure 2). As a result, mullite crystallization commences, which can happen at temperatures as high as 1300 °C. The dispersion of alumina nanoparticles within the polysiloxane is more uniform thanks to the nanoalumina particles. As a result, the finished product comprises a nanostructure composed of mullite crystals measuring 60–160 nm and SiC crystals measuring 1–8 nm.²¹⁰

Mullite's potential worth is bolstered by its usage as a durable protective thermal barrier in high-demand applications such as spaceship heat shields. Bulk nanostructured ceramics and nanocomposites were developed, and the structural properties of these materials piqued people's interest. As a result, a new preceramic polymer production process has been discovered.^{212,213} The usage of polysiloxane-derived Si–OC ceramics in the design of microelectromechanical systems is also highlighted.

■ POLYCARBOSILANE

Several organosilicon polymers have been discovered in recent years, and when they are thermally decomposed, they produce ceramic materials with various proportions of silicon carbide (SiC).²¹⁴ Polycarbosilane is a polymer with an unknown structure that is generated when sodium causes thermal isomerization of Me₂SiCl₂. The material is subsequently pyrolyzed to create Nicalon, the only commercial continuous SiC fiber with a micron-sized diameter.²¹⁵ Polycarbosilane has been the most widely utilized polymeric precursor for SiC ceramics since Yajima et al.'s pioneering work on SiC fibers.^{218–220} Polycarbosilanes are made by heating polydimethylcarbosilane under high pressure in an autoclave to produce polyphenylcarbosilane (see Figure 3).²¹⁷

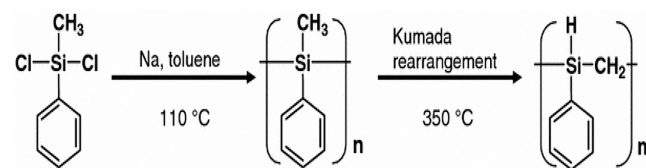


Figure 3. Preparation process of polyphenylcarbosilane using toluene and sodium.

Although a variety of linear polysilanes²¹⁶ and polycarbosilanes and toluene²²¹ have been developed, they are not excellent SiC precursors because they depolymerize and provide little or no ceramic yield when heated. To boost ceramic production, the polymer must have heat cross-linking capabilities.

For catalytic processes, Hasegawa et al. created solid acid catalysts such as AlCl₃, MnCl₂, CrCl₃, VCl₃, TiCl₄, and GaCl₃.²²³ When these catalysts are used, the molecular weight of the polycarbosilane generated is too low, resulting in poor spinnability for PCS fiber manufacture. This could be due to the high acidity of metal chloride catalysts. If the solid acid catalyst is tuned to have adjustable acidity, it appears that an efficient solid acid catalyst for the Kumada rearrangement can be created. The vibration bands of polycarbosilane generated by a catalytic method match the functional groups of polycarbosilane. The band is quite strong, indicating polycarbosilane synthesis, and it is caused by the Si–CH₂–Si group's CH₂ bending vibration.²²²

■ BLOCK COPOLYMER

A copolymer is a polymer that contains a variety of monomers. Copolymerization is the process of polymerizing monomers into copolymers. Biopolymers are copolymers formed by copolymerizing two monomer types. Block copolymers are polymers made up of alternating segments of diverse polymer compositions joined by reactive ends. Block copolymers are made up of two or more homopolymer subunits joined by covalent connections.

When compared to traditional microstructures and bulk materials, the ability to change ceramic structure on the nanoscale allows us to produce innovative and/or better characteristics and functions.^{224–227} Nanoscale ordered ceramics with customized pore size, high specific surface area, and increased durability have received a lot of attention in the previous decade.^{229,230} Membrane, battery, and catalytic applications gain from tailored pore size and high specific surface area, whereas ceramic structural applications profit from improved toughness.

Because of their capacity to self-assemble on the nanoscale into well-defined and structured nanostructures, block copolymers (BCPs) are an interesting template material.²²⁸ Unfavorable monomers, that is, monomer interactions, cause self-assembly of the different polymer blocks, which frequently necessitates a heat and/or solvent annealing phase. Preceramic polymers (PCPs) are frequently employed as a ceramic precursor in the BCP self-assembly process due to their chemical modularity and ease of processing.^{231–234} By combining PCPs with BCPs, a soft templating technique for making nanostructured ceramics has been developed, as well as bespoke synthesis of BCPs incorporating PCP blocks. Due to the limited phases accessible by BCPs, only a few studies have employed this method to construct three-dimensional and connected nanostructures. The utilization of the self-assembly of block copolymers to template ceramic nanostructures is well-known, but their mechanical properties have yet to be studied.^{233,234}

The use of functionalized benzoyl peroxide as the polymerization initiator in the manufacture of PVDF (poly(vinylidene fluoride))-based block copolymers is a synthetic method. ¹H NMR is frequently used to confirm the effective synthesis of chlorine-terminated P (VDF-TrFE). The single-atom-based catalyst is additionally supported by silicon carbide or nitride in this approach. This preceramic carbide is more stable and aids in the prevention of coking during catalytic processes.²³¹

■ TECHNIQUES FOR SI-BASED PRECERAMIC POLYMER SYNTHESIS

Shape Memory Synthesis. Ledoux and co-workers devised a new synthetic approach called shape memory synthesis (SMS) for creating medium surface area -SiC containing binders a few years ago to overcome the drawbacks of commercially available SiC, which has a very low surface area -SiC including binders.^{56,57} The SMS-prepared SiC was found to be an excellent catalyst support for a variety of reactions, including hydrodesulfurization and oxidation,⁵⁷ isomerization of linear saturated hydrocarbons,⁵² selective oxidation of hydrogen sulfide into elemental sulfur,⁵⁸ and three-way exhaust catalysts.^{59,60}

For use as a catalyst support, SiC generated by SMS possesses a variety of intriguing and practical properties: (i) a high thermal conductivity compared to more typical supports like alumina or silica, which can prevent metal sintering by keeping the active site temperature under strict control, (ii) chemical inertness allows for easy recovery of active phases like noble metals from spent catalysts using acidic or basic washing treatments, eliminating the need for harsh techniques like those utilized with alumina-based spent catalysts, and (iii) SiC-based catalysts have a high mechanical strength and thermal stability, making them resistant to erosion and attrition.⁵⁵

A few years ago, shape memory synthesis was employed to synthesize large-specific-surface-area SiC.^{59,61} Owing to the unavailability of bulk oxygen in its structure, its ability to disperse different active phases demonstrated in other catalytic applications,⁵⁸ and its high thermal conductivity, which should greatly contribute to the reaction's heat management, this material had been an outstanding candidate to support the single atom catalyst.

Wet Polymer Spinning Approach. The wet polymer spinning approach for carbon nanofibers (CNFs) (Table 1) has gotten a lot of attention in recent years.⁶⁸ Making carbon nanofibers by electrospinning a carbon precursor polymer solution and then thermally treating them was a standard method. Polyimide,⁶⁹ polyacrylonitrile (PAN),⁷⁰ and phenolic resin are being used as carbon precursor polymers.⁷¹ In a nonsolvent coagulation bath, the polymer is disseminated in a spinning solvent and squeezed out using a spinneret. As a result of the coagulation bath, the polymer precipitates as fibers. Acrylic, rayon, aramid, modacrylic, and Spandex are all made using this approach.

Among these polymers, phenolic resin produces carbonized fibers with a high microporosity and a large carbon yield without the use of activation.⁶⁹ Fiberizing uncured phenolic resins and then implementing a sequential carbonization procedure to cure the as-spun fibers with a cross-linking agent was the general technique for constructing phenolic-resin-derived CNFs.

Due to preceramic polymers' unique features, such as carbon nanofibers, and the simplicity with which they can be electrospun, porous carbon nanofibers have significant characteristics as compared to preceramic polymers made up of carbon-containing nanofibers, such as ultrahigh specific surface area, highly developed pore structure, and outstanding adsorption performance.⁷¹ Porous carbon nanofibers are hence great candidates for a wide range of applications. Until recently, the most often used precursor for carbonizing electrospun nanofibers was polyacrylonitrile. However, electrospun porous carbon nanofibers have a low carbonization yield, and porous

Table 1. Selected Properties of Shape Memory and Wet Polymer Spinning Synthetic Schemes

	Shape Memory Synthesis	Wet Polymer Spinning Synthesis	References
Surface area	a. Very low surface area α -SiC b. Medium surface area β -SiC c. Large-specific-surface-area SiC	Ultrahigh specific surface area	56, 57, 61
Mechanical strength and weakness	High mechanical strength	Electrospun porous carbon nanofiber yield is very low	68
Oxidation performance	Its activity is very effective when used as catalyst support in: a. Hydrodesulfurization and oxidation b. Isomerization of saturated compounds c. Oxidation of hydrogen sulfide d. Oxidation of <i>n</i> -butane	a. Excellent adsorption in the process b. Oxidation of methane c. Oxidation of soot	52, 58, 61, 72
Common precursors used	Polyimide	a. Polyimide b. Polyacrylonitrile c. Phenolic resin	69–71
Phase separation	There is phase separation	Significant phase separation	74
Active phases	a. Ability to disperse different active phases b. Easy recovery of active phases	Ability to disperse phase domains	55, 58, 74

carbon nanofibers have a solid interior and smooth surface, resulting in a small specific surface area and almost no pores, limiting their application potential.

Electrospinning is a great way to make nanofibers from polymers or composite materials because it is so simple and versatile. Specifically, significant research has proven that nanoporous fibers can be created by adjusting suitable electrospinning parameters, with the underlying assumption being based on how phase separation processes occur during electrospinning.^{72,73} Internal holes can be created if there is enough phase difference between two polymers for one of them to scatter in the matrix of one another, and the dispersed phase is accessible and removable. Electrospinning bicomponent polymer systems, according to the theory, can produce ultrafine bicomponent fibers with significant phase separation, and selective removal of the dispersed phase domains can result in intrafiber holes.⁷⁴

Plasma-Assisted Oxidation Approach. Preceramic polymers such as silicon carbide have the potential for extraordinary performance in powered electronic devices due to features such as a wide bandgap and a strong electric breakdown field, making it suitable for high-power and high-frequency metal-oxide semiconductor devices with minimal power loss.^{116–119} Because of the large density of interface traps at the PCP interface, photo-aided carbides built on 4H-carbide exhibit extraordinarily low inversion-channel mobilities.^{120–124}

The most frequent method for producing high-quality SiO₂ films is thermal oxidation. Due to the long duration and high temperatures required to manufacture SiO₂ on SiC substrates in a furnace, the oxidation process creates a lot of thermal stress, resulting in a thicker transition area and the creation of defects at the SiO₂/SiC interface.^{18,125,127,128,129} As a result,

during the thermal oxidation process, the interface between a SiO₂ gate and a SiC substrate degrades more than a SiO₂ gate manufactured on a Si substrate. Defect growth during high-temperature oxidation creates bulk traps, which limit the mobility of 4H-SiC-based catalysts, according to numerous studies.^{126,130,131} Additionally, an abundance of C atoms near the SiC substrate's interface causes the formation of SiO_xC_y species because of a reaction involving O₂ and di-interstitial C clusters formed by the pairing of interstitial C atoms, which is one of the main reasons for the SiC substrate's poor oxidation performance.^{132–134}

On SiC substrates, the properties of SiO₂ films produced at room temperature via direct plasma-assisted oxidation were examined.¹¹⁵ The generation of SiO_xC_y species in the transition zones of thermally grown (Figure 4a) and plasma-

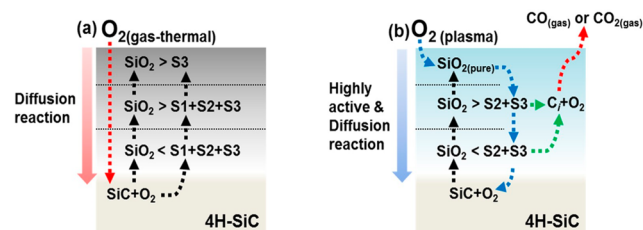


Figure 4. Schematic diagram of the reaction mechanisms involved in the (a) thermal and (b) plasma-assisted oxidation processes. Reproduced with permission from ref 115. Copyright Nature, 2016.

assisted (Figure 4b) SiO₂ films differs dramatically, according to a combination of experimental data and theoretical calculations. The plasma-assisted oxidation approach appears to be particularly beneficial in improving the electrical properties of SiO₂/SiC systems, according to the findings of this study, due to lower SiO_xC_y species concentrations and relatively stable interface states.

The unstable Si–O–C network structure can be disrupted by plasma-assisted oxidation, allowing degraded Si and Si–O to mix with plasma and produce the more stable SiO₂.¹³⁵ The SiO₂ layer becomes more stable as the highly active O plasma comes into contact with fault areas in the SiO₂ layer. C-based byproducts are evaporated simultaneously during the plasma-assisted oxidation process by reacting with decomposed C and C–O.

Bae and Lucovsky evaluated the possibility of subcutaneous oxidation of GaN throughout plasma-enhanced deposition of SiO₂ films using Auger electron spectroscopy data. They discovered that SiO₂ deposition has an independent effect on GaN–GaO_x interface development, resulting in much lower defect state concentrations at the GaN–SiO₂ interface.¹³⁶ Plasma-enhanced deposition consumes plasma-activated O species at a faster rate than continuous oxidation at the buried Si–SiO₂ contact in SiH₄ deposition processes.^{137,138}

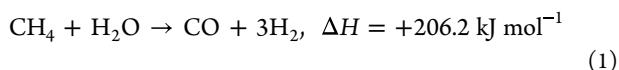
OXIDATION MECHANISMS OF PRECERAMIC POLYMER-BASED CATALYSTS

Catalysis and Oxidation–Reduction. A catalyst interacts with chemical reactants to speed up the process. Catalysts combine with reactants to generate transitory intermediate chemical compounds, allowing the reaction to pursue a different mechanistic path with a lower activation energy (*E_a*) than a noncatalyzed process. By stabilizing the transition state by generating an intermediate species with one of the

reactants, catalysts allow the reaction to proceed more quickly. As products are generated, the catalyst also replenishes itself.²⁰³

An oxidation reaction is a chemical reaction in which electrons are transferred between two substances. Any chemical reaction in which the oxidation number of a molecule, atom, or ion changes by gaining or losing an electron is known as an oxidation–reduction reaction. The real or formal transfer of electrons across chemical entities, with one species experiencing oxidation and the other undergoing reduction, is defined as an oxidation–reduction process. The potential charge of an atom in its ionic state is represented by oxidation numbers. The oxidation number of an atom lowers in a process, and it is reduced. When an atom's oxidation number rises, it is said to be oxidized.

Oxidation of Methane via Si-Derived Preceramic Polymer Catalysts. Conversion of CH₄ into hydrocarbons and other useful products is tricky due to the need for an energy-demanding endothermic reaction process. The existing industrial strategy is to use a catalyst to convert CH₄ into a mixture of H₂ and CO.^{38,39} There has been an increase in the investigation into oxidation of methane catalysis, and there has been surprisingly little work on the oxidation of methane exploiting preceramic polymer catalyst as a support material. Integrating Si-derived preceramic polymer support materials with the ability to exhibit tunable morphology or structure, which then have excellent stability and thermal conductivity and chemically resistant surfaces to coke build-up, is one unique way to minimize coke formation during the oxidation of methane.²⁵¹ The active phase, catalyst loading, precursor and support, calcination temperature, catalyst pretreatment, and reaction conditions all influence catalyst behavior.³⁹ Catalyst supports such as preceramic polymers, silica, and alumina have two functions: they help with effective dispersion of an expensive active phase, and they give mechanical strength. However, by changing or reacting with other catalytic components, the support can help catalytic activity to some extent. Phase change, surface and volume diffusion, sintering, and contact with the active phase are all ways for the support to deactivate the catalyst. Preceramic polymers are used in a variety of chemical processing industries and applications. Clean fuel based on oxidation is crucial in sectors such as chemical recovery and purification. Nonoxide ceramics such as SiC and SiCN have been proposed as precursors for silicon-derived polymers with nitrogen, carbon, and boron.²⁵⁰ Steam reforming is commonly used to convert methane.^{1,40–42} The reaction is strongly endothermic, as shown in eq 1, and normally occurs at higher temperatures.



The conversion of CH₄ into syngas is primarily accomplished via the steam reforming of methane (SRM) reaction (eq 1) where the CH₄ reacts with steam at high temperature (800–900 °C) in the presence of a catalyst.²⁵¹ An alternative to SRM is the dry reforming of methane (DRM) reaction (eq 2) where the H₂O is replaced by CO₂. The DRM has the advantage of being an effective carbon capture and utilization (CCU) strategy, although it suffers from a high level of carbon formation, ultimately leading to catalyst deactivation. In any case, both reactions are endothermic in nature, requiring a high and continual energy input for them to proceed.

Based on catalytic partial oxidation data, there has been a discovery that ionic platinum is more effective for the activation of methane.⁴⁰ The entire study looked at bulk materials, which have disadvantages in terms of cost, heat transmission, and catalyst stability at high temperatures. As supports for high-temperature catalytic processes, Frind and colleagues developed large-surface-area silicon carbide materials³⁷ (see Figure 5). Silicon carbide is remarkably stable in decreasing circumstances, and its strong heat conductivity inhibits the formation of hot spots.^{42,43}

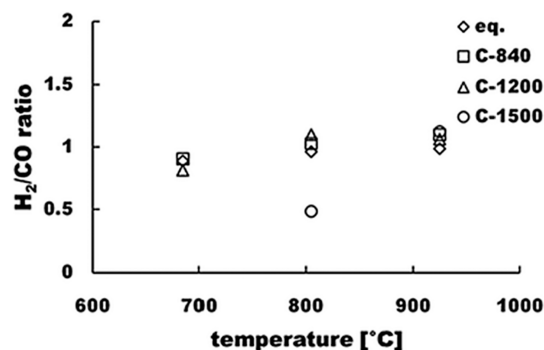


Figure 5. H₂/CO ratio for the dry reforming of methane with composition C at different pyrolysis conditions. Reproduced with permission from ref 37. Copyright 2012, Royal Society of Chemistry.

Several methods for manufacturing highly porous SiC materials, as well as Ce/Pt catalysts supported on SiC for methane oxidation and diesel soot oxidation, have been developed in refs 46 and 47. Using the previously described preceramic polymer SiC production, the partial oxidation activity of methane was investigated by refs 45 and 47. During the synthesis process, the catalyst particles are generated in the water phase, and the polymeric polycarbosilane precursor is transported to the oil phase. Carbon residues were removed by oxidative treatment after pyrolysis at various temperatures to create ceramic silicon carbide, resulting in porous silicon oxycarbide composites. These composites have a large specific surface area and good partial oxidation and dry reforming capabilities for methane.

A third element, such as oxygen, nitrogen, boron, titanium, aluminum, or zirconium, can be added to the SiC network to create a variety of SiC-based materials with improved properties.⁴⁴ The complex-covalent chemical connections produced in silicon oxycarbide (SiOC) and carbonitride (SiCN) ceramics, for example, improve oxidation.

Garca-Vargas and colleagues⁴⁸ investigated how the order of Ni and Mg impregnation affects the catalytic activity and stability of β-SiC-aided methane trireformation catalysts. The initial Ni impregnation showed the lowest catalytic performance, which was most likely due to a weak interaction between Ni and Mg, possible Ni particle obstruction by Mg particles, and the subsequent production of Ni₂Si. Smaller Ni particle sizes reduced coke rate generation, and enhanced basicity and Ni–Mg interaction were identified in catalysts with the highest Mg/Ni molar ratio. Because of its high catalytic activity, stability, and minimal coke generation, Ni–Mg/SiC was chosen as the best catalyst.

Silicon carbide-based catalysts have been found to exhibit high thermal conductivity, oxidation resistance, mechanical strength, chemical inertness, and average surface area.⁵¹

Although SiC-based catalysts have demonstrated good methane trireforming performance,^{48–50} their catalytic stability, particularly their resistance to coke deactivation, should be explored before they are considered as promising catalysts for this process. The optimum promoter for Ni/SiC catalysts employed in the methane trireformation process was discovered to be Mg.⁴⁸ Mg increased the activity and stability of the catalyst, resulting in smaller Ni metal particles and higher basicity.

Methivier and co-workers recently revealed that β -SiC can be used as a substrate for palladium particles in the complete oxidation of methane, with β -SiC being the most thermally conducting solid on which palladium can be placed as small particles using chemical procedures.^{52–54} Light-off temperatures ranged from 330 to 470 °C when low hourly space velocities were used, demonstrating that the preparation procedure changed the catalytic activity and thermal stability.

Oxidation of Methane to Formaldehyde on Preceramic Polymer-Based Catalysts. Oxidation of methane to formaldehyde is one of the most successful cleaning procedures due to its capacity to effectively break down tough organic particles as well as its multiple benefits such as low energy consumption, no additional pollution, and user friendliness.

There has been a revitalization in the oxidation of methane to formaldehyde reaction, fueled by advances in catalyst materials, catalyst makeup, and synthesis strategies; enhanced analytical and modeling capabilities; and the potential to harness “other” material properties using nonthermal energy inputs. Advances in material development have seen the introduction of nonconventional catalyst supports like preceramic polymers. Preceramic polymers have the capability to offer greater resistance to coke formation. Crucial to the feasibility of these materials is the availability of innovative synthesis strategies where past hurdles such as intrinsically low surface areas have been addressed. In relation to the active preceramic polymer-based catalyst, high dispersion across the support may also be a path to better performance.

At ambient pressure, several studies on the selective oxidation of methane to formaldehyde over heterogeneous catalysts have been published.^{63–65} Methanol is rarely found among the reaction products under these conditions unless the input gas is given a large amount of steam.⁶⁶ A few mechanistic investigations have also been published. Even though the two main catalyst systems in this challenge, molybdenum oxide on silica and vanadium oxide on silica, use different approaches, they have a lot in common.

According to the observations, when a mixture of CH₄ and ¹⁸O₂ interacts with MoO₃/SiO₂, the resulting HCHO comprises almost entirely ¹⁶O, which is eliminated from the lattice.⁶⁶ The species that causes the first activation of methane to form the methyl radical, adsorbed oxygen, or lattice oxygen, as well as the phase in the mechanism where oxygen is introduced into the hydrocarbon, have both been a source of debate.

Kartheuser and Hodnett⁶² used the preliminary approach of temporal analysis of products to report the results of research of methane oxidation to formaldehyde over a vanadium oxide catalyst supported on a remarkable preceramic polymer, silica. Since methane has a poor interface with the catalyst surface, but oxygen has a strong affinity, it is hypothesized that an adsorbed oxygen species is involved in the first activation of methane. To make formaldehyde, lattice oxygen is removed

after the creation of methyl radicals in the first stage. Kartheuser and Hodnett⁶² also discovered that methanol was never present during oxidation reactions and that formaldehyde was completely converted into HCH¹⁶O when the oxidant ¹⁸O₂ was applied. The catalyst and ¹⁸O₂ exchanged very little information, which is compatible with the reaction network below:

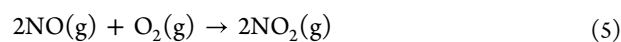


Results from the laboratory of ref 67 show that molybdenum supported on silica is an excellent catalyst for the partial oxidation of methane to methanol and formaldehyde when nitrous oxide is present as the oxidant. The researchers' combination of selectivity and activity has never been duplicated in a current investigation.⁶⁷ Liu and colleagues used kinetic data to determine how the selective oxidation pathway fits into the bigger picture.^{66,67} This selective mechanism is supported by spectroscopic evidence of the production of methyl radicals and methoxide ions on the surface.

It has been formerly described that transparent, free-standing films can be obtained when tetraethoxysilane is polymerized in situ in a poly(methyl methacrylate) (PMMA) binder under certain conditions.²⁵³ These molecular composites exhibit excellent mechanical properties at temperatures extending far above the glass transition temperature of PMMA, consistent with a reinforcing, interacting inorganic network that has not phase separated from the organic polymer. Sol-gel methodology was employed to synthesize V/SiO₂ catalysts by using tetraethoxysilane, poly(methyl methacrylate), and vanadium acetylacetonate, and this catalyst preparation methodology was chosen because of its simplicity. Preceramic polymer (poly(methyl methacrylate)) helps to limit the formation of coke during the oxidation reaction and to achieve a better control of the particle size and morphology of the active phase.²⁵² A high space velocity results in a lower CH₄ conversion and promotes HCHO formation. In summary, the high yield of formaldehyde was attributed to the preceramic polymer due to its chemical stability and ability to prevent the formation of coke.

Soot Oxidation over Preceramic Polymer-Based Catalysts. Diesel engines emit soot, which is hazardous to the environment. Soot is a respiratory threat because it often contains adsorbed polycyclic aromatic hydrocarbons (PAHs). When carbonaceous fuels are burned under local reducing circumstances, soot can develop. Its oxidation is required to minimize pollution in industrial fires and automobile engines. Because the primary products, reaction order, and activation energy all change in the catalyzed soot reaction, the process is different. Decreased ignition temperatures result from lower activation energy and improved reactivity.

The final examination of typical diesel soot was done when the soot had been degassed for 5 h at 150 °C and 13 mPa.^{22–24} Sulfur was visible on the surface as adsorbed compounds (sulfates), while oxygen was tightly bound. The presence of C=O, C–O–C, and C–OH bonds, as well as certain aromatic compounds, was discovered using FTIR.²¹





In a fluidized bed reactor, soot oxidation over noble metal supported on preceramic polymer-based catalysts was examined, with RuO_x/SiO₂ displaying the maximum activity. In a fluidized bed reactor, NO_x was degraded or transformed to N₂ and N₂O, with NO₂ oxidizing much of the soot. The dissociation of adsorbed NO on the Ru oxide surface, which was hindered in the presence of soot because soot oxidation devoured adsorbed NO and NO₂, was linked to the decomposition or transition of NO_x to N₂ or N₂O. Soot oxidation was facilitated by the formation of adsorbed NO and NO₂, which have a higher oxidizing activity. RuO_x/SiO₂ performed better in a fluidized bed reactor than soot oxidation in a fixed bed reactor. The active species' high mass transfer during fluidization is responsible for the high activity in a fluidized bed reactor.

While passing through a preceramic polymer-based catalyst, the concentration of NO₂ generated is always lowered, which is not the case in a fixed bed reactor (Figures 6b and 6c). The significant mass transfer can be explained by the consumption of NO₂ in the soot oxidation reaction (eqs 2–5). NO will be oxidized to NO₂ (eq 6) because of the decrease in NO₂ during soot oxidation (eq 5). Catalytic oxidation can speed up the combustion of soot. This is performed by coating the filter surface with a catalyst, most commonly preceramic-based catalysts, which reduces the danger of operation and energy consumption.^{25,28}

Carbon dioxide prevented soot production primarily by chemical involvement in flames, according to refs 26–32. According to Liu and colleagues' numerical simulations of coflow diffusion flames,^{33–36} the hydroxyl radicals formed by hydrogen atoms reacting with carbon dioxide increased the oxidation of soot precursors.

Preceramic polymer combustion is a difficult process to understand. Polymers inside liquid droplet bulk are likely to experience cross-linking, scissoring, and thermal degradation when exposed to the intense heat and radiation of combustion.^{254,255} Thermal breakdown of a polymer chain causes primary valence bonds to rupture, resulting in a decreased overall molecular weight and smaller components.²⁵⁶ These smaller components, which are mainly methane and C_{2–4} hydrocarbons,^{257–259} burn more quickly than their parent components. As a result of variables such as greater thermal degradation and heat conductivity, preceramic polymers have higher overall combustion rates in blends with either crude oil or natural gas. PCP may suffer from less thermal degradation due to its chain length, but it is effective at reducing diffusion of lighter crude ends through the liquid bulk and lowering surface evaporation rates from the droplet surface, resulting in a lower overall combustion rate in blends with either crude.

Singh and his colleagues investigated the impact of preceramic polymer on combustion characteristics and soot deposits (Singh et al., 2021). The results demonstrated that several combustion parameters such as combustion rate, ignition delay, total combustion time, and flame stand-off ratio are affected by both polymer chain length and crude oil origin. In addition, when compared to the base fuel, preceramic polymeric additives affected the soot deposit structure and particle size.²⁶⁰

Carbon Black Oxidation. Carbon black is mostly oxidized by a simple and clean air calcination method to introduce

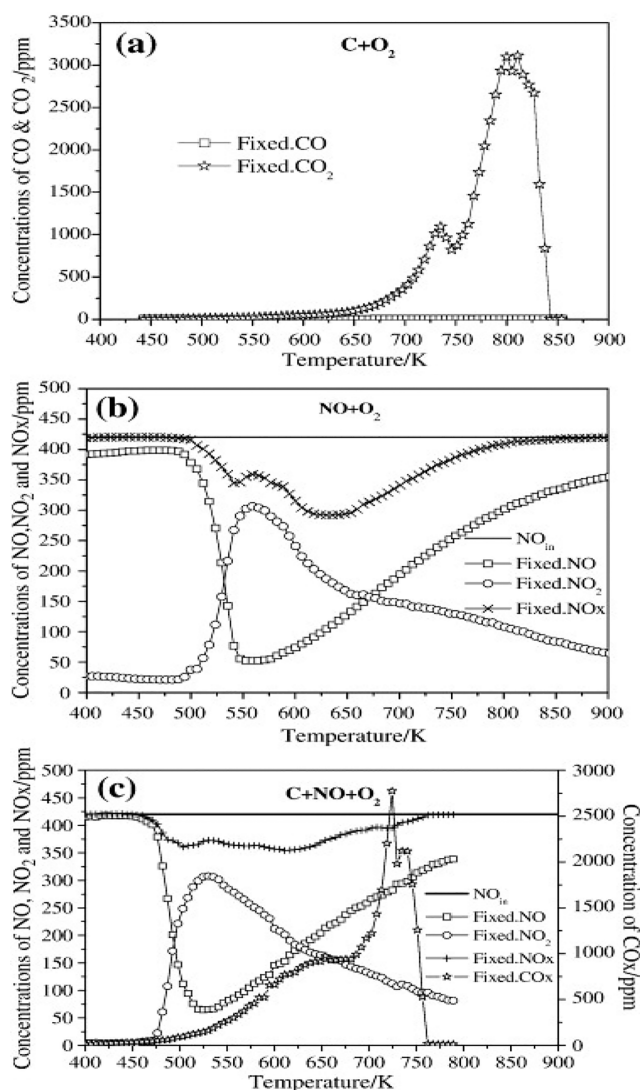


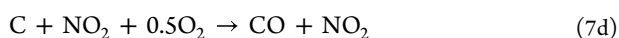
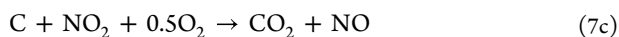
Figure 6. TPR results over RuO_x/SiO₂ in fixed bed reactor under different reactant conditions: (a) C + 4.4 vol % O₂ + Ar; (b) 420 ppm of NO + 4.4 vol % O₂ + Ar; and (c) C + 420 ppm of NO + 4.4 vol % O₂ + Ar. Catalyst weight = 0.2 g, soot weight = 0.02 g, flow rate = 150 mL/min. Reproduced with permission from ref 25. Copyright Elsevier, 2013.

oxygen functional groups to its surface, activating the electrocatalytic and catalytic ability of a conduction band toward the 2e⁻ oxygen reduction rate. Most catalysts supported on alumina, silica, or silicon carbide (synthesized from preceramic polymer-based precursor) have been investigated for the carbon black oxidation capability by introduction of oxygen functional groups.^{10–12} A Ru-based catalyst supported on a PCP based substrate has a high carbon black oxidation activity because active oxygen species can develop on its surface. When active oxygen species are applied to the carbon surface, carbon oxidation occurs.¹³

Preceramic polymers exhibit remarkable microstructural stability that changes according to pyrolysis temperature investigated. Introduction of carbonaceous phases to preceramic polymers is an effective approach to produce C-rich ceramic composites using a pyrolysis route with a wide range of interests, once the dispersion of the dispersed phase makes it relatively easy to produce precursors in the liquid state before

the heating step.²⁶¹ Carbon black incorporated into Si-containing polymeric precursors enhances the electrical conductivity and electrochemical performance of mechanical, thermal, and oxidation properties of preceramic polymer-based catalysts.²⁶¹

In the absence of a catalyst, the global mechanism of the C–NO₂–O₂ reaction^{14,15} consists of two basic reactions: a direct reaction between carbon and NO₂ (eqs 7c and 7d) and a cooperative reaction between O₂ and NO₂ (eqs 6a and 6b). The following is an example of a global mechanism:

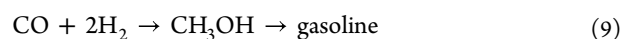
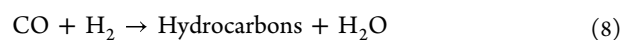


The oxidation rate of a preceramic polymer-based catalyst is boosted in the presence of water vapor.¹³ Small amounts of nitric and nitrous acid are created throughout the operation, resulting in an increase in nitro-oxygenated species on the carbon surface.¹⁵ The ability to create preceramic polymers for carbon black oxidation utilizing plastic-forming processes is one of the primary advantages of their production. Preceramic polymers are best suited for the fabrication of small-dimensioned objects, such as fibers, films, microscopic parts,¹⁶ and thin-walled foams because the polymer–carbon black conversion occurs with a large shrinkage, weight loss, and associated gas release, which often lead to the formation of cracks and porosity.^{17,18} The recommended approach has a few advantages over preceramic microtubes in the case of black carbon oxidation, including its inherent low cost, flexibility, capacity to create complex forms, and wide variety of sizes.^{19,20}

Catalytic Production of Hydrogen. Hydrogen is well-known for a few uses, such as hydrogen-powered forklift trucks, and it is used in fuel cells to create electricity and power cars and provide heat and hot water to people.⁸² Steam reforming of methane and the use of feedstocks such as naphtha, heavy oil, and coal to produce hydrogen have been recognized as one of the essential technologies in sustainability. This is due to increased hydrogen demand in petroleum refining processes such as hydrotreating and hydrocracking^{75,76} as well as petrochemical applications such as methanol production,⁷⁷ methanol-to-gasoline conversion,⁷⁸ ammonia production,⁷⁹ and Fischer–Tropsch hydrocarbon synthesis.⁸⁰

To produce hydrogen from water, a mixture of hydrogen-forming active metal and catalytic supports such as preceramic polymer-based silica catalysts is used.⁸² Only the reductive half-reaction of water splitting (that is, the conversion of protons to hydrogen) can be used to produce hydrogen in the presence of a sacrificial reductant (process termed photocatalytic hydrogen evolution reaction). Even though hydrogen is created as a byproduct of naphtha reforming, it is insufficient to meet refinery requirements. The coming environmental movement, combined with hydrogen-deficient crude oils and the decreasing demand for heavy fuel oil, will propel hydrogen use well into the twenty-first century.

Almost all methane transformation methods start with turning it to synthesis gas. The Fischer–Tropsch process (eq 8) can convert synthesis gas to liquid hydrocarbons over transition metals, or it can be converted to methanol and then to gasoline via the methanol-to-gasoline reaction (eq 9):



Self-assembled hydrogen evolution rate systems have a low catalyst turnover number, low quantum yield, and poor stability. Except for the core seed, which was simply made up of a block copolymer integrating a catalyst, the self-assembled nanofibers contained photosensitizers and catalyst moieties in proximity within the shell. Manners and colleagues^{81,95} irradiated nanofibers in methanol with 5% water and triethanolamine as a sacrificial reductant using visible light. To investigate the effect of the photosensitizer/catalyst ratio,⁸¹ compared nanofibers built of photosensitizer–block–copolymer to catalyst–block–copolymer while maintaining nanofiber length and catalyst concentration constant. When the proportion of photosensitizer was increased, the turnover rate increased. This equates to a hydrogen production rate of 0.327 mol h^{−1}, which is higher than previous polymer-based system standards, and a quantum yield of 4.0% for hydrogen generation using 1.34 g of catalytic polymer. Block copolymers with a crystallizable core-forming block and a shell-forming block containing either a cobalt catalyst or a photosensitizer are used to make nanofibers.

Block copolymers were employed to produce tailored nanofiber architectures that work as an integrated, precious metal-free photocatalytic system for hydrogeochemical reactions.^{84–88} At room temperature, the visible-light-driven artificial assembly was shown to be durable, highly efficient, and recyclable.

Polymer dots are very minute and spread evenly in water. This photocatalyst has a larger reaction surface than traditional photocatalysts, enabling for more light to be stored as hydrogen gas. The research group of Haining Tian^{83,89,94} developed a three-component polymer dot. In tests, the particle displayed excellent catalytic efficiency and stability. This study was effective in optimizing a system of triple-component polymer dots to catalyze the conversion of solar energy into hydrogen at a 7% efficiency rate.

Porous conjugated polymers have made great progress as photocatalysts in recent years, with the polymer's structure proving to be one of the most important factors in achieving high performance.^{90–93,96} The required distance for exciton diffusion is minimized by making the linear conjugated polymer particles as small as possible, reducing unwanted exciton annihilation while also increasing the catalytic surface area and improving photocatalytic efficiency. Polymers have been successfully transformed into nanoparticles with sizes smaller than 100 nm using the nanoprecipitation technique.^{99–101} Amphiphilic polymers or surfactants are commonly used to stabilize polymer nanoparticles in water.^{102–105} Polymer dots are a sort of proton-channeled synthetic polymer nanoparticle that is particularly useful for proton reduction.^{106,107} As a result, polymer dots have been employed as photocatalysts with great success, displaying exceptional photocatalytic hydrogen evolution capabilities.^{108–111}

In the field of energy conversion, donor–acceptor copolymerization is a valuable process for fine-tuning the optical and electrical properties of polymers that are still in the early stages of development.^{91,92} In these copolymer systems, the electron density provided by the electron-donating side chains may influence the electronic capabilities of the donor or

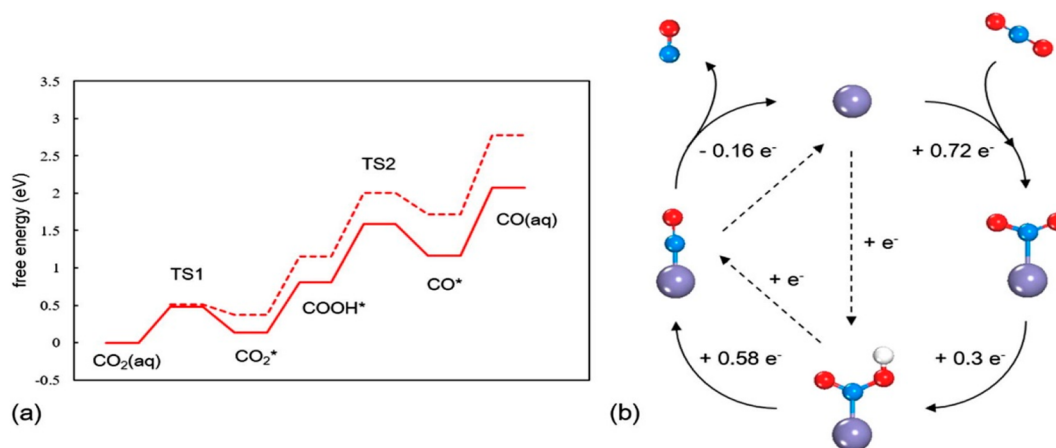


Figure 7. (a) Energy profiles for electroreduction of CO_2 to CO . Solid line indicates the free energy after constant potential corrections, and dashed line indicates the original calculated free energy. (b) Reaction cycles for electroreduction of CO_2 to CO with the calculated electron transfer in every elementary step proposed by the CHE model (dashed arrows) with the electron transfer. Adapted with permission from ref 244. Copyright Elsevier, 2017.

acceptor moieties, as well as the copolymers' physiochemical properties.¹¹²

Antonietti and colleagues developed the most fundamental standard for a graphitic carbon nitride as an organic catalyst for H_2 creation under visible-light-driven conditions.¹¹³ Other organic semiconducting polymers, such as polyazomethine, have been investigated as possible H_2 photocatalysts. Wang's¹¹⁴ group established the importance of microporous organic polymers for photocatalytic performance.

Methanol Synthesis through Oxidation. Methanol is a common industrial chemical used as a starting material to produce other chemicals, most notably formaldehyde, and as a freezing point suppressor for fuel lines. Methanol is made by catalytically hydrogenating carbon monoxide. Catalysts have progressed through several stages of development. Zinc chromium oxide was one of the earliest materials used.^{140,141} Chromium oxide- and aluminum oxide-based catalysts have been introduced.¹³⁹



Even though the reaction appears to be quite simple and of commercial importance, scientists have not completely examined the mechanistic components involved.¹⁴¹ At atmospheric pressure, the reaction's ΔG° becomes negative only at temperatures below 140°C .¹⁴⁵ The critical activity of today's catalysts, however, requires temperatures higher than this. Thermodynamics, kinetics, and mass transfer of the liquid phase methanol synthesis process were previously studied by Lee and colleagues.^{142–144} Based on the actual results obtained for the liquid-phase methanol synthesis process in a mechanically agitated slurry reactor, a computer model program was constructed. It is capable of simulating the rates of all chemical species involved in the process.

CO_2 Photoreduction. The basic principle of CO_2 photoreduction catalysis occurs when the energy of the photons is enough to promote the electrons in the valence band to jump to the conduction band. This occurs in three steps, which include:

- Photon absorption and electron–hole pair generation.
- Charge separation and migration to surface reaction sites or to recombination sites.

(c) Surface chemical reaction at active sites containing donor oxidation at the valence band hole and acceptor reduction at the electron center.

In total, charge from an excited molecule can be injected into the conduction band of a preceramic polymer-based catalyst during catalysis to produce a cation radical.¹⁵⁷ The properties of porous materials like preceramic polymers are influenced by their relative density and morphology or the size and distribution of pores. Depending on the fabrication method, the porosity quality and CO_2 reduction can be altered.¹⁶⁸ Porous ceramics are predicted to be made in a variety of ways, allowing for efficient CO_2 reduction using preceramic polymer-based catalysts.¹⁶⁹

Most catalysts create CO as their primary product, and their activity is identical with catalyst supports like PCP, silica, and alumina. Despite several attempts to understand reaction pathways and interpret activity and selectivity trends, the mechanism of the reaction as well as the source of the exceptional catalytic performance remain a mystery. On the catalyst sites, the steps described below (eqs 10a–10e and Figure 7) are typically included in projected CO_2 to CO reactions:



where $*$ denotes the active site on the catalyst surface.

Also, a proton-decoupled electron transfer process can be described; thus, $* \text{COOH}$ is produced in two steps:

(1) CO_2 adsorption by one-electron transfer to generate an adsorbed CO_2 intermediate (eq 10b) and (2) protonation of the adsorbed CO_2 intermediate to produce $* \text{COOH}$ (eq 10c).^{114,243–245} Whether a $* \text{CO}_2$ intermediate is created directly through a connected proton–electron transfer or indirectly through an electron transfer is the difference between these two processes.

On the path of CO₂ photoreduction, irradiation is a typical start-up route for CO₂ conversion leveraging preceramic polymer-based catalysis, which needs the excitation of electrons by photons at the ground state. In most materials deposited on the PCP surface, such as dye-sensitized solar cells, the excitation step, i.e., light stimulation of electrons at the ground state, proceeds on a periodic basis.^{158–162} Several of the specialized preceramic polymer-based catalysts are primarily used in suspension and electrode systems for water splitting and oxidation/reduction.^{163,164,202} Due to the fact that the final supply of electrons and protons for CO₂ reduction must be H₂O because the burning of a hydrogenated carbon product creates water, using preceramic polymer-based catalysts to convert CO₂ into fuels like methanol and formic acid could help cut CO₂ emissions while also meeting rising energy demands.^{165,166}

Furthermore, controlling the form and size of nanostructured catalysts can improve their activity, selectivity, and stability. The size of catalysts has a direct effect on catalytic activity and selectivity in catalytic processes like CO₂ reduction because the number of low coordinated sites on small catalysts increases with decreasing catalyst size.^{246,247} PCP-based catalysts would have crucial catalytic properties that distinguish them from bulk atoms due to their discrete electronic structure, low coordination surrounding, and finite size effects.²⁴⁸ Catalysts have outperformed their bulk counterparts due to their greater surface areas, offering more active sites for CO₂ adsorption and beginning redox reactions.^{97–99,249}

Electrochemical and Catalytic Reduction of CO₂.

Chemical hydrogenation, cyclic carbonate/carbamate synthesis, and olefin carboxylation, as well as amine methylation and amide generation, have all been attempted recently.^{146,147} CO₂ can also be electrochemically reduced to release formic acid and carbon monoxide as reduction products.¹⁴⁸ One concern is that reversing the CO₂-producing combustion processes involves the use of noncombustion energy sources. Electrochemical energy is one such input that drives the hunt for CO₂ reduction strategies based on electrochemistry. Photoelectrochemical cells powered by the sun, transition metal catalysts, and semiconducting layered double hydroxide catalysts are some of the technologies being researched.¹⁴⁹ In terms of both capture and reduction, organic electrochemical catalysts have not been researched as completely as their transition metal supported on preceramic polymer counterparts.¹⁵⁰ High-energy radical anion aromatics, tetraalkylammonium, and the pyridinium ion are among the targets.¹⁵⁰

Since these intended formamide products are flexible molecules and crucial building components, the formylation of amines with CO₂ (see Figure 8) is an important reaction.

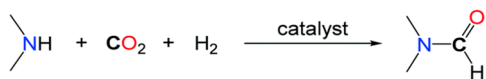


Figure 8. Formylation of amines with CO₂ during CO₂ reduction.

Formic acid, formaldehyde, methanol, and methane can all be made by reducing CO₂ with hydrogen in a series of steps. Despite the favorable thermodynamics of CO₂/H₂ methanol synthesis, the first reduction of CO₂ to formic acid is a difficult operation.^{146,147}

From an electrochemical standpoint, the significant negative voltage required to commence CO₂ reduction is crucial.¹⁵³

The one-electron reduction of CO₂ to CO₂^{•-} has a formal potential of -1.90 V.^{148,152} Even though the theoretical reduction potentials for multiple electron CO₂ reductions are far less negative, every electron transfer from the outer sphere must first go through this severe reduction. This emphasizes the need of developing electrocatalysts that can reduce multiple electrons via inner-sphere pathways.¹⁵³

For pyridine-based polymers, irreversible electrochemically induced carboxylation is favored; however, creating a weak adduct with bipyridine polymer increases CO₂ reduction electrocatalytically, according to Smith and Pickup.¹⁵² When it comes to CO₂ reduction, pyridine-based polymers frequently react irreversibly with dissolved CO₂ to produce an apparently stable product with stable electrochemical activity. Carboxylation produced by electrochemistry is well understood. In acetonitrile containing 1% H₂O, a bipyridine-based polymer functions similarly, with strong catalytic currents for CO₂ reduction.¹⁵²

The amino functional group has been found to be useful in the electrochemical embellishment of electrodes for CO₂ reduction.^{154–156} Essential functions for grafting catalysts have been developed: electrochemical oxidation for the construction of a C–N bond directly with the amino group (Figure 9) and electrochemical reduction for the generation of a C–C bond with the matching diazonium ions formed from the amino group.

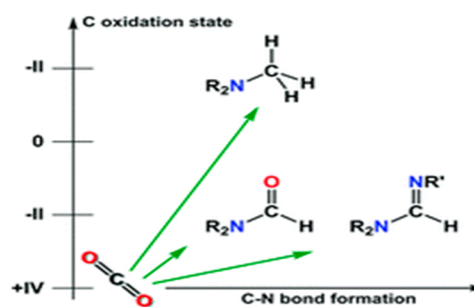


Figure 9. Formylation of N–H bonds with CO₂. Reproduced with permission from ref 147. Copyright Royal Society of Chemistry, 2015.

The development of highly active, long-lasting catalysts for the electrochemical reduction of CO₂ to CH₄ in aqueous media is a cost-effective and environmentally friendly solution to the world's energy and sustainability problems. In aqueous solutions, CO₂ conversion to chemical feedstocks and fuels^{236,237,242} is a useful technique for utilizing CO₂ and lowering greenhouse gas emissions.²³⁶ Because of its compatibility with current infrastructure and potential as a fossil fuel substitute, methane, one of the most major catalytic reductions of CO₂ products, has attracted a lot of attention.²³⁷ Candidate materials for catalyzing CO₂ reduction to CH₄ based on single inorganic atoms, including Au, Co, carbon, Cu, and Cu-based compounds, and catalyst-based supports such as silica, PCP, and alumina have been carefully explored.^{238–242} Han and colleagues²³⁵ designed a single-atom-based catalyst with Zn atoms supported on microporous N-doped carbon to enable multielectron transfer in the CO₂ to CH₄ electrochemical reaction. This catalyst has a high Faradaic efficiency of 85%, indicating far superior performance to dominant Cu-based catalysts for ERC to CH₄. According to theoretical calculations, single Zn atoms primarily impede CO synthesis while assisting CH₄ production.

Antioxidation Ability of Si-Derived Preceramic Polymers. In industries like aerospace engineering, PCP's low oxidation resistance under high-temperature oxidizing conditions has been shown in several studies to have a significant impact on the material's service life, making it an urgent obstacle to deploying PCP products in the above harsh settings. As a result, some studies are concentrating their efforts on producing PCP that is resistant to oxidation at high temperatures.^{177–179} Several investigations have shown that an oxidation-resistant coating with high reflectivity and low conductivity insulation is a suitable solution for safeguarding a substrate at high temperatures.^{104,151,172,173,180,181}

Ren et al.¹⁷¹ discovered that Si₂ has excellent high-temperature permanence and oxidation resistance as well as the ability to sustain performance after exposure to air. As a result, Si₂ is widely regarded as the best antioxidation coating material. However, due to its high coefficient of thermal expansion and quick oxidation, its applications as an antioxidation coating material are limited.^{173,174} According to preliminary studies,¹⁷⁵ adding Si₃N₄ to Si₂ could boost its antioxidation effectiveness at low temperatures. Furthermore, Si₃N₄ may reduce the coefficient of the thermal expansion gap between the substrate and the coating, reducing the risk of thermal cycling-induced coating cracking.

Selective Si oxidation characterizes the oxidation of MoSi₂. With enough SiO₂, a dense film of SiO₂ can be formed, effectively acting as a barrier against oxygen attacks on the matrix. The smooth materials between the particles also aid in keeping the coating compact and preventing oxidation of the matrix.¹⁷⁰ Deep Si infiltration into the C/C substrate and the interaction between Si and C generate the SiC transition layer, which improves the coating's thermal shock resistance and the interface connection strength between the coating and substrate.¹⁷⁶

Due to its remarkable chemical and thermal stability, low oxygen permeability rate, and good wear resistance, zirconium silicate (ZrSiO₄) has become one of the most important ingredients for creating ceramic glaze layers.^{182,183} Furthermore, because SiC and ZrSiO₄ have similar thermal expansion coefficients, both materials have excellent thermal expansion matching, which prevents stress cracking and improves oxidation resistance. As a result, a catalyst based on preceramic polymers, such as ZrSiO₄, could be a good candidate for generating an antioxidant coating for SiC to improve its oxidation resistance at high temperatures.^{184,185}

Applications and Challenges. Increased fossil fuel usage, on the other hand, is expected to be a major source of concern around the world. In recent years, the global energy mix's average carbon intensity has risen. Oil and gas produce more water, hydrogen, and less CO₂ per unit of heat generated when oxidized and burned using a catalyst and a catalyst with substrates such as PCP, silica, and alumina and then coal. Due to expected breakthroughs in fuel consumption, the global carbon emission rate would increase if the carbon intensity remained at its current level of nearly equal parts coal, oil, and natural gas.

By practically any reasonable calculation, stabilizing atmospheric CO₂ levels at 550 ppm or lower by 2050 will require as much carbon-neutral power as is currently produced from all energy sources combined.¹⁹³ Furthermore, because CO₂ emissions build up over a century, even more carbon-neutral power will be needed by 2050 if it is not implemented now with a gradual ramp up.²⁶²

Water splitting, methane oxidation, and methanol synthesis are all part of a wider conversion to fuel cycle that involves the evolution of oxygen, carbon monoxide, and hydrogen as one component as well as the formation of a reduced fuel as a final product.^{263,264} Complete conversion is a multielectron process that benefits from catalysts like preceramic polymer-based catalysts.¹⁹⁷

Capture, conversion, and storage are all required for alternative fuel production via oxidative processes. Catalysts can help with the oxidation process. The goal is to minimize the cost per watt of provided electricity by a significant amount.^{194–196} Methanol, hydrogen, and formaldehyde are liquid fuels that can be stored, handled, and generated from oil, natural gas, coal, or biomass, meaning that they should be widely available and economical to help reduce the use of electricity and fuel. For a long time, most catalysts have relied on materials such as preceramic polymers, silica, alumina and the likes as a crucial precursor or substrate, dating back to the early days of methanol and methane oxidation research.²⁶⁵

Many areas of material and chemical science, such as solar cell supercapacitors and fuel cells, have also focused on catalysts with preceramic polymers as support.^{266–268} Catalysts have emerged as one of the most appropriate carrier materials and electron collectors for increasing the separation and transfer of photoinduced charge carriers due to their large specific surface area, chemical stability, and high charge carrier mobility. The use of single atom metals in stimulating the dissociative adsorption of methanol and methane has been established in a recent study, with an emphasis on preceramic polymer and the likes as support.^{167,198–201} Due to their large absorption range in the visible light section and long carrier diffusion length, single-atom catalysts using preceramic polymers as support have also been brought to attention for their optoelectronic applications.²⁶⁹

One of the main challenges that faces the field of oxidative catalysis is selectivity and product yield with respect to designing a good catalyst, and currently these issues can impede their function in the petroleum industry and related.^{270,271} Immobilization of metal on a substrate such as PCPs makes it so that the material can be easily removed and recycled. Many immobilization substrates are possible, although achieving the same removal rates and efficiency as suspended metal is the overall goal.

CONCLUSIONS AND PROSPECTS

This article gives the understanding of the use of catalysts made of preceramic polymers to catalyze oxidation reactions including methane, soot, and carbon black oxidation in transforming the petroleum industry. The underlying restriction associated with preceramic polymer-based catalysts' low surface area limits the superior catalytic oxidation capabilities. Newer approaches, such as block copolymer templating and supramolecular moiety insertion, show promise in terms of producing an effective catalyst with greater surface values than usual. Furthermore, approaches in catalyst engineering through preceramic polymer precursor construction and oxidation surface possibilities for mesoporous property upgrades such as longer absorption, efficient thermodynamics, reduced recombination, and rapid charge transfer kinetics are possible.

However, as seen below, translating to an engineering-scale application may necessitate extra research:

- a. Redox systems, which combine water oxidation and reduction, are a typical example of waste to worth production since they can produce hydrogen, methanol, and formaldehyde at a minimal cost. In this area, further trials are expected to be done.
- b. For high-volume applications, the ability to prepare these catalysts in a practical and cost-effective manner is crucial. Complementary reactor designs are necessary to make engineering solutions easier.
- c. A basic feature of industrial pertinency is the restoration of catalytic oxidation activity and catalyst resurgence in continuous process cycles. As a result, techniques such as catalytic coatings and magnetically separable powders can be improved, as well as process improvements to aid coactive adsorption and catalytic action.
- d. The low surface area of preceramic polymer-based catalysts is a fundamental limiting factor for oxidative kinetics. Approaches to leveling permeability established during the synthesis of preceramic polymer-based catalysts, such as block copolymer templating, nanocomposites with porous organic frameworks, and coupling of multiple metals or metal oxides, all require further investigation.
- e. Furthermore, building preceramic polymer-based particles that are receptive to morphology observation, evaluating the oxidative catalysis rationality and efficacy of conventional preceramic synthesis and preparative approaches, and then realizing the functions of different preceramic polymer-based particles in specific instances of viable fuel production, energy utilization, and efficacious adsorption should be considered.

As a result, this study contributes to better knowledge of the various approaches for catalytic oxidative reactions of preceramic polymer-based nanocrystals in the petroleum industry.

AUTHOR INFORMATION

Corresponding Author

Williams Kweku Darkwah – School of Chemical Engineering, Faculty of Engineering, The University of New South Wales, Sydney 2052 NSW, Australia; Department of Biochemistry, School of Biological Sciences, University of Cape Coast, Cape Coast 4P48+59H, Ghana; orcid.org/0000-0003-0287-6965; Email: w.darkwah@unsw.edu.au

Authors

Alfred Bekoe Appiagyei – Department of Chemical and Biological Engineering, Monash University, Melbourne, Victoria 3800, Australia

Joshua B. Puplambu – Department of Biochemistry, School of Biological Sciences, University of Cape Coast, Cape Coast 4P48+59H, Ghana

Complete contact information is available at:
<https://pubs.acs.org/10.1021/acsomega.2c07562>

Notes

The authors declare no competing financial interest.

ACKNOWLEDGMENTS

The authors are grateful for financial support from the American Chemical Society Petroleum Research Fund (ACSPRF).

REFERENCES

- (1) Choudhary, T. V.; Banerjee, S.; Choudhary, V. R. No equilibrium Oxidative Conversion of methane to CO and H₂ with High Selectivity and Productivity over Ni/Al₂O₃ at Low Temperature. *Appl. Catal., A* **2002**, *234*, 1.
- (2) Trimm, D. L. Catalytic Combustion (Review). *Appl. Catal.* **1983**, *7*, 249.
- (3) Pfefferle, L. D.; Pfefferle, W. C. Catalysis in Combustion. *Catalysis Reviews Science and Engineering* **1987**, *29* (2–3), 219–267.
- (4) Ciuparu, D.; Lyubovsky, M. R.; Altman, E.; Pfefferle, L. D.; Datye, A. Catalytic Combustion of Methane Over Palladium-Based Catalysts. *Catalysis Reviews* **2002**, *44* (4), 593–649.
- (5) Ledoux, M. J.; Huu, C. P.; Guille, J.; Dunlop, H. Compared Activities of Platinum and High Specific Surface Area Mo₂C and WC Catalysts for Reforming Reactions I. Catalyst Activation and Stabilization: Reaction of n-Hexane. *J. Catal.* **1992**, *134*, 383–398.
- (6) Ledoux, M. J.; Hantzer, S.; Huu, C. P.; Guille, J.; Desaneaux, M.-P. Catalysis with carbides. *J. Catal.* **1988**, *114*, 176–185.
- (7) Bouchy, C.; Pham-Huu, C.; Heinrich, B.; Chaumont, C.; Ledoux, M. J. Microstructure and Characterization of a Highly Selective Catalyst for the Isomerization of Alkanes: A Molybdenum Oxycarbide. *J. Catal.* **2000**, *190*, 92–103.
- (8) Acres, G. J. K. Platinum Catalysts for the Control of Air Pollution. The Elimination of Organic Fume by Catalytic Combustion. *Plat. Met. Rev.* **1970**, *14*, 2.
- (9) Radcliffe, S. W.; Hickman, R. G. Diffusive catalytic combustors. *J. Inst. Fuel* **1975**, *48*, 208.
- (10) Jeguirim, M.; Villani, K.; Brillhac, J. F.; Martens, J. A. Ruthenium, and platinum catalyzed carbon oxidation: A comparative kinetic study. *Appl. Catal., B* **2010**, *96*, 34–40.
- (11) Jeguirim, M.; Tschamber, V.; Villani, K.; Brillhac, J. F.; Martens, J. A. Mechanistic Study of Carbon Oxidation with NO₂ and O₂ in the Presence of a Ru/NaY Catalyst. *Chem. Eng. Technol.* **2009**, *32*, 830–834.
- (12) Jeguirim, M.; Tschamber, V.; Brillhac, J. F. Kinetics of catalyzed and non-catalyzed soot oxidation with nitrogen dioxide under regeneration particle trap conditions. *J. Chem. Technol. Biotechnol.* **2009**, *84*, 770–776.
- (13) Tschamber, V.; Jeguirim, M.; Villani, K.; Martens, J.; Ehrburger, P. Comparison of the activity of Ru and Pt catalysts for the oxidation of carbon by NO₂. *Appl. Catal., B* **2007**, *72*, 299–303.
- (14) van Setten, B. A. A. L.; Schouten, J. M.; Makkee, M.; Moulijn, J. A. Realistic contact for soot with an oxidation catalyst for laboratory studies. *Appl. Catal., B* **2000**, *28*, 253–257.
- (15) Wilson, M. K.; Badger, R. M. Infrared Spectrum and Force Constants of the Nitrite Ion. *Physics Review* **1949**, *76*, 472–473.
- (16) Liew, L.-A.; Zhang, W.; An, L.; Shah, S.; Luo, R.; Liu, Y.; Cross, T.; Dunn, M. L.; Bright, V.; Daily, J. W.; Raj, R.; Anseth, K. Ceramic MEMS. New Materials, Innovative Processing and Future Application. *Am. Ceram. Soc. Bull.* **2001**, *80* (5), 25–30.
- (17) Maccagnan, G.; Colombo, P. “Method for Producing Micromanufactured Items in Ceramic Materials, and Micromanufactured Items Produced with Said Method,” International Pat. App. No. PCT/IT02/00312, Milan, Italy, May 13, 2002.
- (18) Pantano, C. G.; Singh, A. K.; Zhang, H. X. Silicon Oxycarbide Glasses. *J. Sol-Gel Sci. Technol.* **1999**, *14*, 7–25.
- (19) Sorarù, G. D.; Modena, S.; Guadagnino, E.; Colombo, P.; Egan, J.; Pantano, C. Chemical Durability of Silicon Oxycarbide Glasses. *J. Am. Ceram. Soc.* **2002**, *85* (6), 1529–36.
- (20) Colombo, P.; Perini, K.; Bernardo, E.; Capelletti, T.; Maccagnan, G. Ceramic Microtubes from Preceramic Polymers. *J. Am. Ceram. Soc.* **2003**, *86* (6), 1025–1027.
- (21) Stanmore, B. R.; Brillhac, J. F.; Gilot, P. The oxidation of soot: a review of experiments, mechanisms, and models. *Carbon* **2001**, *39*, 2247–2268.
- (22) Veranth, J. M.; Fletcher, T. H.; Pershing, D. W.; Sarofim, A. F. Measurement of soot and char in pulverised coal fly ash. *Fuel* **2000**, *79*, 1067–75.

- (23) Lahaye, J.; Boehm, P.; Chambion, P.; Ehrburger, P. Influence of cerium oxide on the formation and oxidation of soot. *Combust. Flame* **1996**, *104*, 199–207.
- (24) Marcucilli, F.; Gilot, P.; Stanmore, B. R.; Prado, G. Experimental and theoretical study of diesel soot reactivity. In: *Twenty-fifth international symposium on combustion*; The Combustion Institute: Philadelphia, 1994; pp 619–26.
- (25) Guo, M.; Ouyang, F.; Pang, D.; Qiu, L. Highly efficient oxidation of soot over RuOx/SiO₂ in fluidized bed reactor. *Catal. Commun.* **2013**, *38*, 40–44.
- (26) Mei, J.; You, X.; Law, C. K. Effects of CO₂ on soot formation in ethylene pyrolysis. *Combust. Flame* **2020**, *215*, 28–35.
- (27) Oh, K. C.; Shin, H. D. The effect of oxygen and carbon dioxide concentration on soot formation in non-premixed flames. *Fuel* **2006**, *85*, 615–624.
- (28) Liu, F.; Karatas, A. E.; Gülder, Ö.L.; Gu, M. Numerical and experimental study of the influence of CO₂ and N₂ dilution on soot formation in laminar coflow C₂H₄/air diffusion flames at pressures between 5 and 20 atm. *Combust. Flame* **2015**, *162*, 2231–2247.
- (29) Tang, Q.; Mei, J.; You, X. Effects of CO₂ addition on the evolution of particle size distribution functions in premixed ethylene flame. *Combust. Flame* **2016**, *165*, 424–432.
- (30) Naseri, A.; Veshkini, A.; Thomson, M. J. Detailed modeling of CO₂ addition effects on the evolution of soot particle size distribution functions in premixed laminar ethylene flames. *Combust. Flame* **2017**, *183*, 75–87.
- (31) Schug, K.; Manheimer-Timnat, Y.; Yaccarino, P.; Glassman, I. Sooting behavior of gaseous hydrocarbon diffusion flames and the influence of additives. *Combust. Sci. Technol.* **1980**, *22*, 235–250.
- (32) Karatas, A. E.; Gülder, Ö.L. Effects of carbon dioxide and nitrogen addition on soot processes in laminar diffusion flames of ethylene-air at high pressures. *Fuel* **2017**, *200*, 76–80.
- (33) Liu, F.; Guo, H.; Smallwood, G. J.; Gülder, Ö.L. the chemical effects of carbon dioxide as an additive in an ethylene diffusion flame: implications for soot and NO_x formation. *Combust. Flame* **2001**, *125*, 778–787.
- (34) Chang, Q.; Gao, R.; Li, H.; Yu, G.; Wang, F. Effect of CO₂ on the characteristics of soot derived from coal rapid pyrolysis. *Combust. Flame* **2018**, *197*, 328–339.
- (35) Teini, P. D.; Karwat, D. M.; Atreya, A. The effect of CO₂/H₂O on the formation of soot particles in the homogeneous environment of a rapid compression facility. *Combust. Flame* **2012**, *159*, 1090–1099.
- (36) Abián, M.; Millera, A.; Bilbao, R.; Alzueta, M. Experimental study on the effect of different CO₂ concentrations on soot and gas products from ethylene thermal decomposition. *Fuel* **2012**, *91*, 307–312.
- (37) Frind, R.; Borchardt, L.; Kockrick, E.; Mammitzsch, L.; Petasch, U.; Herrmann, M.; Kaskel, S. Mathias Herrmann, and Stefan Kaskel Complete and Partial oxidation of methane on ceria/platinum silicon carbide nanocomposites. *Catal. Sci. Technol.* **2012**, *2*, 139–146.
- (38) Pena, M.A.; Gomez, J.P.; Fierro, J.L.G. New catalytic routes for syngas and hydrogen production. *Appl. Catal., A* **1996**, *144*, 7–57.
- (39) Christian Enger, B.ør.; Lødeng, R.; Holmen, A. A review of catalytic partial oxidation of methane to synthesis gas with emphasis on reaction mechanisms over transition metal catalysts. *Appl. Catal., A* **2008**, *346*, 1–27.
- (40) Tang, W.; Hu, Z.; Wang, M.; Stucky, G. D.; Metiu, H.; McFarland, E. W. Methane complete and partial oxidation catalyzed by Pt-doped CeO₂. *J. Catal.* **2010**, *273*, 125–137.
- (41) Kochloeff, K. *Handbook of Heterogeneous Catalysis*; Wiley-VCH: Weinheim, Germany, 1997; Vol. 4, pp 1819–1831.
- (42) Colombo, P.; Modesti, M. Silicon Oxycarbide Ceramic Foams from a Pre-ceramic Polymer. *J. Am. Ceram. Soc.* **1999**, *82*, 573–578.
- (43) Shi, Y. F.; Wan, Y.; Zhai, Y. P.; Liu, R. L.; Meng, Y.; Tu, B.; Zhao, D. Y. Ordered Mesoporous SiOC and SiCN Ceramics from Atmosphere-Assisted in Situ Transformation. *Chem. Mater.* **2007**, *19*, 1761–1771.
- (44) Weinmann, M.; Schuhmacher, J.; Kummer, H.; Prinz, S.; Peng, J. Q.; Seifert, H. J.; Christ, M.; Müller, K.; Bill, J.; Aldinger, F. Synthesis and thermal behavior of novel Si-B-C-N ceramic precursors. *Chem. Mater.* **2000**, *12*, 623–632.
- (45) Kockrick, E.; Schrage, C.; Grigas, A.; Geiger, D.; Kaskel, S. Synthesis and Catalytic Properties of Microemulsion-Derived Cerium Oxide Nanoparticles. *J. Solid State Chem.* **2008**, *181*, 1614–1620.
- (46) Kockrick, E.; Krawiec, P.; Petasch, U.; Martin, H. P.; Herrmann, M.; Kaskel, S. Tubular and rodlike ordered mesoporous silicon (oxy)carbide ceramics and their structural transformations. *Chem. Mater.* **2008**, *20*, 77–83.
- (47) Krawiec, P.; Geiger, D.; Kaskel, S. Ordered mesoporous silicon carbide (OM-SiC) via polymer precursor nanocasting. *Chem. Commun.* **2006**, 2469.
- (48) Garcia-Vargas, J. M.; Valverde, J. L.; Diez, J.; Sanchez, P.; Dorado, F. Preparation of Ni–Mg/β-SiC catalysts for the methane tri-reforming: Effect of the order of metal impregnation. *Appl. Catal. B: Environmental* **2015**, *164*, 316–323.
- (49) García-Vargas, J. M.; Valverde, J. L.; De Lucas-Consuegra, A.; Gómez-Monedero, B.; Sánchez, P.; Dorado, F. Precursor influence and catalytic behaviour of Ni/CeO₂ and Ni/SiC catalysts for the tri-reforming process. *Appl. Catal. A: Gen.* **2012**, *431–432*, 49–5.
- (50) García-Vargas, J. M.; Valverde, J. L.; Díez, J.; Sánchez, P.; Dorado, F. Influence of alkaline and alkaline-earth cations on the performance of Ni/β-SiC catalysts in the methane tri-reforming reaction. *Appl. Catal. B: Environ.* **2014**, *148–149*, 322–329.
- (51) Nguyen, D. L.; Leroi, P.; Ledoux, M. J.; Pham-Huu, C. Influence of the oxygen pretreatment on the CO₂ reforming of methane on Ni/b-SiC catalyst. *Catal. Today* **2009**, *141*, 393–396.
- (52) Pham-Huu, C.; Del Gallo, P.; Peschiera, E.; Ledoux, M. J. n-Hexane and n-heptane isomerization at atmospheric and medium pressure on MoO₃-carbon modified supported on SiC and Y₂La₃. *Appl. Catal. A: General* **1995**, *132*, 77–96.
- (53) Methivier, C.; Beguin, B.; Brun, M.; Massardier, J.; Bertolini, J.C. Pd/SiC Catalysts Characterization and Catalytic Activity for the Methane Total Oxidation. *J. Catal.* **1998**, *173*, 374–382.
- (54) Methivier, C.; Massardier, J.; Bertolini, J. C. Pd/Si₃N₄ catalysts: preparation, characterization, and catalytic activity for the methane oxidation. *Appl. Catal., A* **1999**, *182*, 337–344.
- (55) Nhut, J.-M.; Pesant, L.; Keller, N.; Pham-Huu, C.; Ledoux, M. J. Pd/SiC exhaust gas catalyst for heavy-duty engines: improvement of catalytic performances by controlling the location of the active phase on the support. *Top. Catal.* **2004**, *30/31*, 353–358.
- (56) Ledoux, M.J.; Hantzer, S.; Guille, J.; Dubots, D. US Patent No. 4914070, assigned to the Pechiney Electrometallurgie Co. (1990).
- (57) Ledoux, M. J.; Hantzer, S.; Huu, C. P.; Guille, J.; Desaneaux, M.-P. New Synthesis and Uses of High-Specific-Surface SiC as a Catalytic Support that Is Chemically Inert and Has High Thermal Resistance. *J. Catal.* **1988**, *114*, 176–185.
- (58) Keller, N.; Pham-Huu, C.; Crouzet, C.; Ledoux, M. J.; Savin-Poncet, S.; Nougayrède, J.-B.; Bousquet, J. Direct oxidation of H₂S into S. New catalysts and processes based on SiC support. *Catal. Today* **1999**, *53*, 535–542.
- (59) Cuong, P.-H.; Marin, S.; Ledoux, M. J.; Weibel, M.; Ehret, G.; Benaissa, M.; Peschiera, E.; Guille, J. Synthesis and characterization of platinum-rhodium supported on SiC and SiC doped with cerium: Catalytic activity for the automobile exhaust reactions. *Appl. Catal. B: Environ.* **1994**, *4*, 45–63.
- (60) Ledoux, M. J.; Crouzet, C.; Pham-Huu, C.; Turines, V.; Kourtakis, K.; Mills, P. L.; Lerou, J. J. High-Yield Butane to Maleic Anhydride Direct Oxidation on Vanadyl Pyrophosphate Supported on Heat-Conductive Materials: Ø-SiC, Si₃N₄, and BN. *J. Catal.* **2001**, *203*, 495.
- (61) Grindatto, B.; Prin, M. Process for the production of metal carbides having a large specific surface under atmospheric pressure inert gas scavenging. (Pechiney), European Patent 0,548,752A (1992).
- (62) Kartheuser, B.; Hodnett, B. K.; Zanthoff, H.; Baerns, M. Transient experiments on the selective oxidation of methane to

formaldehyde over V2O5/SiO2 studied in the temporal-analysis-of-products reactor. *Catal. Lett.* **1993**, *21*, 209–214.

(63) Kennedy, M.; Sexton, A.; Kartheuser, B.; Mac Giolla Coda, E.; McMonagle, J.B.; Hodnett, B.K. Selective oxidation of methane to formaldehyde: comparison of the role of promoters in hydrocarbon rich and lean conditions. *Catal. Today* **1992**, *13*, 447–454.

(64) Coda, E. M. G.; Hodnett, B. K. *New Developments in Selective Oxidation, Studies in Surface Science and Catalysis*; Centi, G., Trifir, F., Eds.; Elsevier: Amsterdam, 1990; Vol. 55, p 459.

(65) Amiridis, M. D.; Rekoske, J. E.; Dumesic, J. A.; Rudd, D. F.; Spencer, N. D.; Pereira, C. J. Stimulation of Methane Partial Oxidation over silica supported MoO3 and V2O5. *AIChE J.* **1991**, *37*, 87.

(66) Liu, H. F.; Liu, T. S.; Liew, K. Y.; Johnson, R. E.; Lunsford, J. H. Partial oxidation of methane by nitrous oxide over molybdenum on silica. *J. Am. Chem. Soc.* **1984**, *106*, 4117.

(67) Liu, R.-S.; Iwamoto, M.; Lunsford, J. H. Partial oxidation of methane by nitrous oxide over molybdenum oxide supported on silica. *J. Chem. Soc., Chem. Commun.* **1982**, 78.

(68) Wang, M. X.; Huang, Z. H.; Kang, F. Y.; Liang, K. M. Porous carbon nanofibers with narrow pore size distribution from electrospun phenolic resin. *Mater. Lett.* **2011**, *65*, 1875–7.

(69) Chronakis, I. S. J. Novel nanocomposites and nanoceramics based on polymer nanofibers using electrospinning process—a review. *Mater. Process Tech.* **2005**, *167*, 283–293.

(70) Kim, D. K.; Park, S. H.; Kim, B. C.; Chin, B. D.; Jo, S. M.; Kim, D. Y. Electrospun Polyacrylonitrile-Based Carbon Nanofibers and Their Hydrogen Storages. *Macromol. Res.* **2005**, *13*, 521–8.

(71) Zhang, Z. Y.; Li, X. H.; Wang, C. H.; Fu, S. W.; Liu, Y. C.; Shao, C. L. Polyacrylonitrile and Carbon Nanofibers with Controllable Nanoporous Structures by Electrospinning. *Macromol. Mater. Eng.* **2009**, *294*, 673–8.

(72) Bognitzki, M.; Czado, W.; Frese, T.; Schaper, A.; Hellwig, M.; Steinhart, M.; Greiner, A.; Wendorff, J. H. Nanostructured Fibers via Electrospinning. *Adv. Mater.* **2001**, *13*, 70.

(73) Varabhas, J. S.; Chase, G. G.; Reneker, D. H. Electrospun nanofibers from a porous hollow tube. *Polymer* **2008**, *49*, 4226.

(74) Zhang, L.; Hsieh, Y.-L. Nanoporous ultrahigh specific surface polyacrylonitrile fibres. *Nanotechnology* **2006**, *17*, 4416.

(75) Pena, M. A.; Gomez, J.P.; Fierro, J. L. G. New catalytic routes for syngas and hydrogen production. *Appl. Catal. A: General* **1996**, *144*, 7–57.

(76) Prins, R.; de Beer, V. H. J.; Somorjai, G. A. Structure and Function of the Catalyst and the Promoter in Co—Mo Hydrodesulfurization Catalysts. *Catal. Rev.-Sci. Eng.* **1989**, *31*, 1.

(77) Kung, H. H. Methanol Synthesis. *Catal. Rev.-Sci. Eng.* **1980**, *22*, 235.

(78) Chang, C. D. Mechanism of Hydrocarbon Formation from Methanol. *Stud. Surf. Sci. Catal.* **1988**, *36*, 127.

(79) Ozaki, A.; Aika, K. *Catalysis: Science and Technology*; Anderson, J. R., Boudart, M., Eds.; Springer Verlag, New York, 1981; Vol. 1, Chapter 3, p 106.

(80) Rofer-de-Poorter, C. K. A Comprehensive Mechanism for the Fischer—Tropsch Synthesis. *Chem. Rev.* **1981**, *81*, 447.

(81) Tian, J.; Zhang, Y.; Du, L.; He, Y.; Jin, X.-H.; Pearce, S.; Eloi, J.-C.; Hamman, R. L.; Alibhai, D.; Ye, R.; Phillips, D. L.; Manners, I. Tailored self-assembled photocatalytic nanofibres for visible-light-driven hydrogen production. *Nat. Chem.* **2020**, *12*, 1150–1156.

(82) Staffell, I.; Scamman, D.; Velazquez Abad, A.; Balcombe, P.; Dodds, P. E.; Ekins, P.; Shah, N.; Ward, K. R.; et al. The role of hydrogen and fuel cells in the global energy system. *Energy Environ. Sci.* **2019**, *12*, 463–491.

(83) Mao, S. S.; Shen, S. Catalysing artificial photosynthesis. *Nat. Photonics* **2013**, *7*, 944–946.

(84) Wang, X.; et al. cylindrical block copolymer micelles and comicelles of controlled length and architecture. *Science* **2007**, *317*, 644–647.

(85) Arno, M. C.; et al. Precision epitaxy for aqueous 1D and 2D poly(ϵ -caprolactone) assemblies. *J. Am. Chem. Soc.* **2017**, *139*, 16980–16985.

(86) Schöbel, J.; et al. Bottom-up meets top-down: patchy hybrid nonwovens as an efficient catalysis platform. *Angew. Chem., Int. Ed.* **2017**, *56*, 405–408.

(87) Shin, S.; et al. Living light-induced crystallization-driven self-assembly for rapid preparation of semiconducting nanofibers. *J. Am. Chem. Soc.* **2018**, *140*, 6088–6094.

(88) Hailes, R. L. N.; Oliver, A. M.; Gwyther, J.; Whittell, G. R.; Manners, I. Polyferrocenylsilanes: synthesis, properties, and applications. *Chem. Soc. Rev.* **2016**, *45*, 5358–5407.

(89) Liu, A.; Gedda, L.; Axelsson, M.; Pavliuk, M.; Edwards, K.; Hammarstrom, L.; Tian, H. Panchromatic Ternary Polymer Dots Involving Sub-Picosecond Energy and Charge Transfer for Efficient and Stable Photocatalytic Hydrogen Evolution. *J. Am. Chem. Soc.* **2021**, *143*, 2875–2885.

(90) Mikhnenko, O. V.; Blom, P. W. M.; Nguyen, T.-Q. Exciton Diffusion in Organic Semiconductors. *Energy Environ. Sci.* **2015**, *8* (7), 1867–1888.

(91) Zhang, J.-H.; Wei, M.-J.; Wei, Z.-W.; Pan, M.; Su, C.-Y. Ultrathin Graphitic Carbon Nitride Nanosheets for Photocatalytic Hydrogen Evolution. *ACS Appl. Nano Mater.* **2020**, *3* (2), 1010–1018.

(92) Zhang, J.; Chen, J.; Wan, Y.; Liu, H.; Chen, W.; Wang, G.; Wang, R. Defect Engineering in Atomic-Layered Graphitic Carbon Nitride for Greatly Extended Visible-Light Photocatalytic Hydrogen Evolution. *ACS Appl. Mater. Interfaces* **2020**, *12* (12), 13805–13812.

(93) Ting, L.-Y.; Jayakumar, J.; Chang, C.-L.; Lin, W.-C.; Elsayed, M. H.; Chou, H.-H. Effect of Controlling the Number of Fused Rings on Polymer Photocatalysts for Visible-Light-Driven Hydrogen Evolution. *J. Mater. Chem. A* **2019**, *7* (40), 22924–22929.

(94) Ru, C.; Wei, Q.; Chen, W.; Guan, Q.; Zhang, Q.; Ling, Y.; Tao, C.; Qin, D.; Wu, J.; Pan, X. Tunable Conjugated Organoborane Oligomers for Visible-Light-Driven Hydrogen Evolution. *ACS Energy Lett.* **2020**, *5* (2), 669–675.

(95) Dai, C.; Liu, B. Conjugated Polymers for Visible-Light-Driven Photocatalysis. *Energy Environ. Sci.* **2020**, *13* (1), 24–52.

(96) Xiang, Y.; Wang, X.; Rao, L.; Wang, P.; Huang, D.; Ding, X.; Zhang, X.; Wang, S.; Chen, H.; Zhu, Y. Conjugated Polymers with Sequential Fluorination for Enhanced Photocatalytic H2 Evolution via Proton-Coupled Electron Transfer. *ACS Energy Lett.* **2018**, *3* (10), 2544–2549.

(97) Byun, J.; Landfester, K.; Zhang, K. A. I. Conjugated Polymer Hydrogel Photocatalysts with Expandable Photoactive Sites in Water. *Chem. Mater.* **2019**, *31* (9), 3381–3387.

(98) Li, L.; Hadt, R. G.; Yao, S.; Lo, W.-Y.; Cai, Z.; Wu, Q.; Pandit, B.; Chen, L. X.; Yu, L. Photocatalysts Based on Cobalt-Chelating Conjugated Polymers for Hydrogen Evolution from Water. *Chem. Mater.* **2016**, *28* (15), 5394–5399.

(99) Wang, Z.; Mao, N.; Zhao, Y.; Yang, T.; Wang, F.; Jiang, J.-X. Building an Electron Push–Pull System of Linear Conjugated Polymers for Improving Photocatalytic Hydrogen Evolution Efficiency. *Polym. Bull.* **2019**, *76* (6), 3195–3206.

(100) Zhang, X.; Shen, F.; Hu, Z.; Wu, Y.; Tang, H.; Jia, J.; Wang, X.; Huang, F.; Cao, Y. Biomass Nano-micelles Assist Conjugated Polymers/Pt Cocatalysts to Achieve High Photocatalytic Hydrogen Evolution. *ACS Sustainable Chem. Eng.* **2019**, *7* (4), 4128–4135.

(101) Damas, G. B.; Marchiori, C. F. N.; Araujo, C. M. Tailoring the Electron-Rich Moiety in Benzothiadiazole-Based Polymers for an Efficient Photocatalytic Hydrogen Evolution Reaction. *J. Phys. Chem. C* **2019**, *123* (42), 25531–25542.

(102) Woods, D. J.; Hillman, S. A. J.; Pearce, D.; Wilbraham, L.; Flagg, L. Q.; Duffy, W.; McCulloch, I.; Durrant, J. R.; Guilbert, A. A. Y.; Zwiijnenburg, M. A.; Sprick, R. S.; Nelson, J.; Cooper, A. I. Side Chain Tuning in Conjugated Polymer Photocatalysts for Improved Hydrogen Production from Water. *Energy Environ. Sci.* **2020**, *13* (6), 1843–1855.

- (103) Xu, C.; Zhang, W.; Tang, J.; Pan, C.; Yu, G. Porous Organic Polymers: An Emerged Platform for Photocatalytic Water Splitting. *Front. Chem.* **2018**, *6*, 592.
- (104) Wang, L.; Fernandez-Teran, R.; Zhang, L.; Fernandes, D. L. A.; Tian, L.; Chen, H.; Tian, H. Organic Polymer Dots as Photocatalysts for Visible Light-Driven Hydrogen Generation. *Angew. Chem., Int. Ed.* **2016**, *55* (40), 12306–12310.
- (105) Pecher, J.; Mecking, S. Nanoparticles of Conjugated Polymers. *Chem. Rev.* **2010**, *110* (10), 6260–6279.
- (106) Liu, A.; Tai, C.-W.; Hola, K.; Tian, H. Hollow Polymer Dots: Nature-Mimicking Architecture for Efficient Photocatalytic Hydrogen Evolution Reaction. *J. Mater. Chem. A* **2019**, *7* (9), 4797–4803.
- (107) Dai, C.; Pan, Y.; Liu, B. Conjugated Polymer Nanomaterials for Solar Water Splitting. *Adv. Energy Mater.* **2020**, *10*, 2002474.
- (108) Zhao, P.; Wang, L.; Wu, Y.; Yang, T.; Ding, Y.; Yang, H. G.; Hu, A. Hyperbranched Conjugated Polymer Dots: The Enhanced Photocatalytic Activity for Visible Light-Driven Hydrogen Production. *Macromolecules* **2019**, *52* (11), 4376–4384.
- (109) Tseng, P.-J.; Chang, C.-L.; Chan, Y.-H.; Ting, L.-Y.; Chen, P.-Y.; Liao, C.-H.; Tsai, M.-L.; Chou, H.-H. Design and Synthesis of Cyclo-platinated Polymer Dots as Photocatalysts for Visible-Light Driven Hydrogen Evolution. *ACS Catal.* **2018**, *8* (9), 7766–7772.
- (110) Fortin, P.; Rajasekar, S.; Chowdhury, P.; Holdcroft, S. Hydrogen Evolution at Conjugated Polymer Nanoparticle Electrodes. *Can. J. Chem.* **2018**, *96* (2), 148–157.
- (111) Rahman, M. Z.; Kibria, M. G.; Mullins, C. B. Metal-Free Photocatalysts for Hydrogen Evolution. *Chem. Soc. Rev.* **2020**, *49* (6), 1887–1931.
- (112) Chang, C.-L.; Lin, W.-C.; Jia, C.-Y.; Ting, L.-Y.; Jayakumar, J.; Elsayed, M. H.; Yang, Y.-Q.; Chan, Y.-H.; Wang, W.-S.; Lu, C.-Y.; Chen, P.-Y.; Chou, H.-H. Low-toxic cycloplatinated polymer dots with rational design of acceptor comonomers for enhanced photocatalytic efficiency and stability. *Appl. Catal. B: Environmental* **2020**, *268*, 118436.
- (113) Wang, Y.; Wang, X.; Antonietti, M. Polymeric Graphitic Carbon Nitride as a Heterogeneous Organocatalyst: From Photochemistry to Multipurpose Catalysis to Sustainable Chemistry. *Angew. Chem., Int. Ed.* **2012**, *51*, 68–89.
- (114) Wang, Z.; Yang, X.; Yang, T.; Zhao, Y.; Wang, F.; Chen, Y.; Zeng, J. H.; Yan, C.; Huang, F.; Jiang, J.-X. Dibenzothiophene Dioxide Based Conjugated Microporous Polymers for Visible-Light-Driven Hydrogen Production. *ACS Catal.* **2018**, *8*, 8590–8596.
- (115) Kim, D.-K.; Jeong, K.-S.; Kang, Y.-S.; Kang, H.-K.; Cho, S. W.; Kim, S.-O.; Suh, D.; Kim, S.; Cho, M.-H. Controlling the defects and transition layer in SiO₂ films grown on 4H-SiC via direct plasma-assisted oxidation. *Sci. Rep.* **2016**, *6*, 34945.
- (116) Choyke, W. J.; Matsunami, H.; Pensl, G. *Silicon Carbide: Recent Major Advances*; Springer: Berlin, Heidelberg, NY, 2004.
- (117) Deng, H.; Endo, K.; Yamamura, K. Competition between surface modification and abrasive polishing: a method of controlling the surface atomic structure of 4H-SiC (0001). *Sci. Rep.* **2015**, *5*, 8947.
- (118) Phan, H. P.; et al. Thickness dependence of the piezoresistive effect in p-type single crystalline 3C-SiC nanoscale thin films. *J. Mater. Chem. C* **2014**, *2*, 7176–7179.
- (119) Sugita, T.; Hiramatsu, K.; Ikeda, S.; Matsumura, M. Fabrication of pores in a silicon carbide wafer by electrochemical etching with a glassy-carbon needle electrode. *ACS Appl. Mater. Interfaces* **2013**, *5*, 2580–2584.
- (120) Cheong, K. Y.; Dimitrijević, S.; Han, J.; Harrison, H. B. Electrical and physical characterization of gate oxides on 4H-SiC grown in diluted N₂O. *J. Appl. Phys.* **2003**, *93*, 5682–5686.
- (121) Dhar, S.; Feldman, L. C.; Wang, S.; Isaacs-Smith, T.; Williams, J. R. Interface trap passivation for SiO₂/ (0001) C-terminated 4H-SiC. *J. Appl. Phys.* **2005**, *98*, 014902–014906.
- (122) Lai, P. T.; Chakraborty, S.; Chan, C. L.; Cheng, Y. C. Effects of nitridation and annealing on interface properties of thermally oxidized SiO₂/SiC metal–oxide–semiconductor system. *Appl. Phys. Lett.* **2000**, *76*, 3744–3746.
- (123) Afanas'ev, V. V.; Stesmans, A. Interfacial defects in SiO₂ revealed by photon stimulated tunneling of electrons. *Phys. Rev. Lett.* **1997**, *78*, 2437–2440.
- (124) Afanas'ev, V. V.; Bassler, M.; Pensl, G.; Schulz, M. Intrinsic SiC/SiO₂ Interface States. *Phys. Status Solidi A* **1997**, *162*, 321–337.
- (125) Chang, K.-C.; et al. High-resolution elemental profiles of the silicon dioxide/4H-silicon carbide interface. *J. Appl. Phys.* **2005**, *97*, 104920–104925.
- (126) Hornetz, B.; Michel, H.-J.; Halbritter, J. Oxidation and 6H-SiC–SiO₂ interfaces. *J. Vac. Sci. Technol.* **1995**, *A13*, 767–771.
- (127) Onneby, C.; Pantano, C. G. Silicon oxycarbide formation on SiC surfaces and at the SiC/SiO₂ interface. *J. Vac. Sci. Technol.* **1997**, *A15*, 1597–1602.
- (128) Hijikata, Y.; Yaguchi, H.; Yoshikawa, M.; Yoshida, S. Composition analysis of SiO₂/SiC interfaces by electron spectroscopic measurements using slope-shaped oxide films. *Appl. Surf. Sci.* **2001**, *184*, 161–166.
- (129) Soukiasian, P.; Amy, F. Silicon carbide surface oxidation and SiO₂/SiC interface formation investigated by soft X-ray synchrotron radiation. *J. Electron Spectrosc. Relat. Phenom.* **2005**, *144–147*, 783–788.
- (130) Correa, S. A.; et al. Effects of nitrogen incorporation on the interfacial layer between thermally grown dielectric films and SiC. *Appl. Phys. Lett.* **2009**, *94*, 251909–251911.
- (131) Muller, D. A.; et al. The electronic structure at the atomic scale of ultrathin gate oxides. *Nature* **1999**, *399*, 758–762.
- (132) Zheleva, T.; et al. Transition layers at the SiO₂/SiC interface. *Appl. Phys. Lett.* **2008**, *93*, 022108–022110.
- (133) Shen, X.; Pantelides, S. T. Identification of a major cause of endemically poor mobilities in SiC/SiO₂ structures. *Appl. Phys. Lett.* **2011**, *98*, 053507–053509.
- (134) Zhu, Q.; Huang, L.; Li, W.; Li, S.; Wang, D. Chemical structure study of SiO₂/4H-SiC (0001) interface transition region by angle-dependent x-ray photoelectron spectroscopy. *Appl. Phys. Lett.* **2011**, *99*, 082102–082104.
- (135) Yasuhara, S.; et al. Impact of film structure on damage to low-k SiOCH film during plasma exposure. *J. Phys. D: Appl. Phys.* **2009**, *42*, 235201–235208.
- (136) Bae, C.; Lucovsky, G. Low-temperature preparation of GaN–SiO₂ interfaces with low defect density. I. Two-step remote plasma-assisted oxidation-deposition process. *J. Vac. Sci. Technol. A* **2004**, *22*, 2402–2410.
- (137) Schoder, D. K. *Semiconductor Material and Device Characterization*, 2nd ed.; Wiley: New York, 1998.
- (138) Nicollian, E. H.; Brews, J. R. *MOS (Metal Oxide Semiconductor) Physics and Technology*; Wiley: New York, 1982.
- (139) Stull, D. R.; Westrum, E. F., Jr.; Sinke, G. C. *The Chemical Thermodynamics of Organic Compounds*; Wiley: New York, 1969.
- (140) Rossini, F. D.; et al. Selected Values of Chemical Thermodynamic Properties. *Natl. Bur. Stand. (U. S.), Circ.* **1952**, *500*.
- (141) Vijayaraghavan, P.; Lee, S. Modeling of a Mechanically Agitated Slurry Reactor for Liquid Phase Methanol Synthesis Process. *Fuel Science & Technology International* **1994**, *12* (9), 1221–1243.
- (142) Lee, B. G. "Post-treatment and Regeneration of Industrial Coprecipitated Methanol Synthesis Catalyst". *Ph.D. Dissertation*. The University of Akron, 1989.
- (143) Lee, S.; Parameswaran, V. R.; Sawant, A. V. Mass Transfer in the Liquid Phase Methanol Synthesis Process. AP-5758 Electric Power Research Institute: Palo Alto, California, 1988.
- (144) Lee, S.; Parameswaran, V. R.; Wender, I.; Kulik, C. I. The Roles of Carbon Dioxide in Methanol Synthesis. *Fuel Sci.* **1989**, *7* (8), 1021–1057.
- (145) Lee, S. *Methanol Synthesis*; CRC Press, Inc.: Boca Raton, Florida, 1990.
- (146) Denning, D. M.; Thum, M. D.; Falvey, D. E. Photochemical Reduction of CO₂ Using 1,3-Dimethylimidazolidene. *Org. Lett.* **2015**, *17*, 4152–4155.
- (147) Tlili, A.; Blondiaux, E.; Frogneux, X.; Cantat, T. Reductive functionalization of CO₂ with amines: an entry to formamide,

- formamidine and methylamine derivatives. *Green Chem.* **2015**, *17*, 157–168.
- (148) Benson, E. E.; Kubiak, C. P.; Sathrum, A. J.; Smieja, J. M. electrocatalytic and homogeneous approaches to conversion of CO₂ to liquid fuels. *Chem. Soc. Rev.* **2009**, *38*, 89–99.
- (149) Barton, E. E.; Rampulla, D. M.; Bocarsly, A. B. Selective Solar-Driven Reduction of CO₂ to Methanol Using a Catalyzed p-GaP Based Photoelectrochemical Cell. *J. Am. Chem. Soc.* **2008**, *130*, 6342–6344.
- (150) Oh, Y.; Hu, X. Electrocatalytic Efficiency Analysis of Catechol Molecules for NADH Oxidation during Nanoparticle Collision. *Chem. Soc. Rev.* **2013**, *42*, 2253–2261.
- (151) Boston, D. J.; Xu, C.; Armstrong, D. W.; Macdonnell, F. M. Photochemical Reduction of Carbon Dioxide to Methanol and Formate in a Homogeneous System with Pyridinium Catalysts. *J. Am. Chem. Soc.* **2013**, *135*, 16252–16255.
- (152) Smith, R. D.L.; Pickup, P. G. Nitrogen-rich polymers for the electrocatalytic reduction of CO₂. *Electrochem. Commun.* **2010**, *12*, 1749–1751.
- (153) Bard, A. J. Inner-Sphere Heterogeneous Electrode Reactions. Electrocatalysis and Photocatalysis: The Challenge. *J. Am. Chem. Soc.* **2010**, *132*, 7559.
- (154) Elgrishi, N.; Griveau, S.; Chambers, M. B.; Bedioui, F.; Fontecave, M. Versatile functionalization of carbon electrodes with a polypyridine ligand: metalation and electrocatalytic H⁺ and CO₂ reduction. *Chem. Commun.* **2015**, *51*, 2995–2998.
- (155) Zhou, X.; Micheroni, D.; Lin, Z. K.; Poon, C.; Li, Z.; Lin, W. B. Graphene-Immobilized *fac*-Re(bipy)(CO)₃Cl for Syngas Generation from Carbon Dioxide. *ACS Appl. Mater. Interfaces* **2016**, *8*, 4192–4198.
- (156) Mohamed, E. A.; Zahran, Z. N.; Naruta, Y. Efficient Heterogeneous CO₂ to CO Conversion with a Phosphonic Acid Fabricated Cofacial Iron Porphyrin Dimer. *Chem. Mater.* **2017**, *29*, 7140–7150.
- (157) Nasr, C.; et al. Environmental photochemistry on semiconductor surfaces. Visible light induced degradation of a textile diazo dye, naphthol blue black, on TiO₂ nanoparticles. *J. Phys. Chem.* **1996**, *100*, 8436–8442.
- (158) Nosaka, Y.; Nosaka, A. Y. Generation and Detection of Reactive Oxygen Species in Photocatalysis. *Chem. Rev.* **2017**, *117*, 11302–11336.
- (159) Adormaa, B. B.; Darkwah, W. K.; Ao, Y. Oxygen vacancies of the TiO₂ nano-based composite photocatalysts in visible light responsive photocatalysis. *RSC Adv.* **2018**, *8*, 33551.
- (160) Darkwah, W. K.; Ao, Y. Mini Review on the structural and properties (photocatalysis), preparation techniques of graphite Carbon Nitride (g-C₃N₄) Nano-Based particle. *Nanoscale research letters.* *Nature Springer* **2018**, *13*, 388.
- (161) Hollmann, D.; Karnahl, M.; Tschierlei, S.; Kailasam, K.; Schneider, M.; Radnik, J.; Grabow, K.; Bentrup, U.; Junge, H.; Beller, M.; et al. Structure-Activity Relationships in Bulk Polymeric and Sol-Gel-Derived Carbon Nitrides during Photocatalytic Hydrogen Production. *Chem. Mater.* **2014**, *26*, 1727–1733.
- (162) Li, T.; Zhao, L.; He, Y.; Cai, J.; Luo, M.; Lin, J. Synthesis of g-C₃N₄/SmVO₄ composite photocatalyst with improved visible light photocatalytic activities in RhB degradation. *Appl. Catal. B Environ.* **2013**, *129*, 255–263.
- (163) Reza Gholipour, M.; Dinh, C.-T.; Beland, F.; Do, T.-O. Nanocomposite heterojunctions as sunlight-driven photocatalysts for hydrogen production from water splitting. *Nanoscale* **2015**, *7*, 8187–8208.
- (164) Nakamura, I.; Negishi, N.; Kutsuna, S.; Ihara, T.; Sugihara, S.; Takeuchi, K. Role of oxygen vacancy in the plasma treated TiO photocatalyst with visible light activity for NO removal. *J. Mol. Catal. A: Chem.* **2000**, *161*, 205–212.
- (165) Li, K.; An, X.; Park, K. H.; Khraisheh, M.; Tang, J. A critical review of CO₂ photoconversion: Catalysts and reactors. *Catal. Today* **2014**, *224*, 3–12.
- (166) Hsu, H. C.; Shown, I.; Wei, H. Y.; Chang, Y. C.; Du, H. Y.; Lin, Y. G.; Tseng, C. A.; Wang, C. H.; Chen, L. C.; Lin, Y. C.; Chen, K. H. Graphene oxide as a promising photocatalyst for CO₂ to methanol conversion. *Nanoscale* **2013**, *5*, 262–268.
- (167) Darkwah, W. K.; Teye, G. K.; Ao, Y. Nanoparticles - Graphene Nanocrystals in CO₂ Photo-reduction with H₂O for Fuel Production. *Nanoscale Adv.* **2020**, *2*, 991.
- (168) Kim, Y.-W.; Kim, S.-H.; Xu, X.; Choi, C.-H.; Park, C. B.; Kim, H.-D. Fabrication of porous preceramic polymers using carbon dioxide. *Journal Of Materials Science Letters.* **2002**, *21*, 1667–1669.
- (169) Sakka, Y.; Suzuki, T. S. Textured Development of Feeble Magnetic Ceramics by Colloidal Processing Under High Magnetic Field. *J. Ceram. Soc. Japan.* **2005**, *113*, 26.
- (170) Niu, F.-x.; Wang, Y.-x.; Abbas, I.; Fu, S.-l.; Wang, C.-g. A MoSi₂-SiOC-Si₃N₄/SiC antioxidation coating for C/C composites prepared at relatively low temperature. *Ceram. Int.* **2017**, *43*, 3238–3245.
- (171) Ren, X.; Li, H.; Fu, Q.; Chu, Y.; Li, K. TaB₂-SiC-Si multiphase oxidation protective coating for SiC-coated carbon/carbon composites. *J. Eur. Ceram. Soc.* **2013**, *33*, 2953–2959.
- (172) Sharif, A. A. Effects of Nb-alloying on high-temperature oxidation of MoSi₂. *Acta Phys. Polym.* **2014**, *125*, 563–566.
- (173) Huang, Y.; Lin, J.; Zhang, H. Effect of Si₃N₄ content on microstructures and antioxidant properties of MoSi₂/Si₃N₄ composite coatings on Mo substrate. *Ceram. Int.* **2015**, *41*, 13903–13907.
- (174) Zhang, L.; Pan, K.; Duan, L.; Lin, J. Oxidation behavior of in situ synthesized MoSi₂-SiC composites at 500 °C. *Acta Metall. Sin.* **2013**, *49*, 1303–1310.
- (175) Hebsur, M. G. Development and characterization of SiC(f)/MoSi₂-Si₃N₄(p) hybrid composites. *Mater. Sci. Eng., A* **1999**, *261*, 24–37.
- (176) Fu, Q.; Li, H.; Li, K.; Tong, K. A Si-Mo-W coating to protect SiC-coated carbon/carbon composites against oxidation. *J. Am. Ceram. Soc.* **2009**, *92*, 2132–2135.
- (177) Shi, W. Y.; Liu, B. R.; Deng, X. Y.; Li, J. B.; Yang, Y. X. In-situ synthesis, and properties of cordierite-bonded porous SiC membrane supports using diatomite as silicon source. *J. Eur. Ceram. Soc.* **2016**, *36*, 3465–3472.
- (178) Facciotti, M.; Boffa, V.; Magnacca, G.; Jørgensen, L. B.; Kristensen, P. K.; Farsi, A.; Konig, K.; Christensen, M. L.; Yue, Y. Deposition of thin ultrafiltration membranes on commercial SiC microfiltration tubes. *Ceram. Int.* **2014**, *40*, 3277–3285.
- (179) Deng, W.; Yu, X.; Sahimi, M.; Tsotsis, T. T. highly permeable porous silicon carbide support tubes for the preparation of nano porous inorganic membranes. *J. Membr. Sci.* **2014**, *451*, 192–204.
- (180) Wang, P.; Zhou, C. L.; Zhang, X. H.; Zhao, G. D.; Xu, B. S.; Cheng, Y. H.; Zhou, P.; Han, W. B. (ZrB₂-SiC)/SiC oxidation protective coatings for graphite materials. *Ceram. Int.* **2016**, *42*, 2654–2661.
- (181) Huang, J. F.; Wang, B.; Li, H. J.; Liu, M.; Cao, L. Y.; Yao, C. Y. A MoSi₂/SiC oxidation protective coating for carbon/carbon composites. *Corros. Sci.* **2011**, *53*, 834–839.
- (182) Schelz, S.; Branland, N.; Plessis, D.; Minot, B.; Guillet, F. Laser treatment of plasma sprayed ZrSiO₄ coatings. *Surf. Coat. Technol.* **2006**, *200*, 6384–6388.
- (183) Kaiser, A.; Lobert, M.; Telle, R. Thermal stability of zircon (ZrSiO₄). *J. Eur. Ceram. Soc.* **2008**, *28*, 2199–2211.
- (184) Yao, X. Y.; Li, H. J.; Zhang, Y. L.; Wu, H.; Qiang, X. F. A SiC-Si-ZrB₂ multiphase oxidation protective ceramic coating for SiC-coated carbon/carbon composites. *Ceram. Int.* **2012**, *38*, 2095–2100.
- (185) He, R. J.; Zhang, R. B.; Zhu, X. L.; Wei, K.; Qu, Z. L.; Pei, Y. M.; Fang, D. N. improved green strength and green machinability of ZrB₂-SiC through gel casting based on a double gel network. *J. Am. Ceram. Soc.* **2014**, *97*, 2401–2404.
- (186) Wang, X.; Schmidt, F.; Hanaor, D.; Kamm, P. H.; Li, S.; Gurlo, A. Additive manufacturing of ceramics from preceramic polymers: A versatile stereolithographic approach assisted by thiol-ene click chemistry. *Additive Manufacturing* **2019**, *27*, 80–90.

- (187) Fritz, G. Synthesis of organosilicon compounds. V. Thermal decomposition of tetramethyl- and tetraethylsilicon. *Z. Anorg. Allg. Chem.* **1956**, *286*, 149.
- (188) Xia, Y.; Whitesides, G. M. Soft Lithography. *Annu. Rev. Mater. Sci.* **1998**, *28*, 153.
- (189) Xia, Y.; Rogers, J. A.; Paul, K. E.; Whitesides, G. M. Unconventional Methods for Fabricating and Patterning Nanostructures. *Chem. Rev.* **1999**, *99*, 1823.
- (190) Kim, E.; Xia, Y.; Whitesides, G. M. Micromolding in Capillaries: Applications in Materials Science. *J. Am. Chem. Soc.* **1996**, *118*, 5722–7863.
- (191) Nguyen, N. T.; Wereley, S. T. *Fundamentals and Applications of Microfluidics*; Artech House: Boston, 2002; pp 82–97.
- (192) Madou, M. J. *Fundamentals of Microfabrication - The Science of Miniaturization*, 2nd ed.; CRC Press: Boca Raton, 2002; pp 519–521.
- (193) United Nations Development Program. *World Energy Assessment Report: Energy and the Challenge of Sustainability*; United Nations: New York, 2003.
- (194) Moniz, E.; Deutch, J., Eds. *The Future of Nuclear Power*; Massachusetts Institute of Technology: Cambridge, MA, USA, 2003.
- (195) Metz, B.; Davidson, O.; de Coninck, L. H. M.; Meyer, L., Eds. *Carbon Dioxide Capture and Storage*; Intergovernmental Panel on Climate Change: Washington, DC, USA, 2005.
- (196) Solar Energy Utilization Workshop. *Basic Science Needs for Solar Energy Utilization*; US Dept of Energy: Washington, DC, 2005.
- (197) Lewis, N. S.; Nocera, D. G. Powering the planet: Chemical challenges in solar energy utilization. *Proc. Natl. Acad. Sci. USA* **2006**, *103*, 15729–15735.
- (198) Lima; Coutanceau, C.; LeGer, J.-M.; Lamy, C. Investigation of ternary catalysts for methanol electrooxidation. *J. Appl. Electrochem.* **2001**, *31*, 379–386.
- (199) Lamy, C.; Léger, J.-M. Advanced electrode materials for the direct methanol fuel cell. In *Interfacial Electrochemistry. Theory, Experiment, and Applications*; Wieckowski, A., Ed.; Marcel Dekker, Inc., New York, 1999; p 885, Ch. 48.
- (200) Arico, A. S.; Baglio, V.; Antonucci, V. Direct methanol fuel cells: history, status, and perspectives. In *Electrocatalysis of Direct Methanol Fuel Cells: from Fundamentals to Applications*; Liu, H., Zhang, J., Eds.; Wiley-VCH Verlag GmbH & Co. KGaA: Weinheim, 2009; pp 3–9, Ch. 1.
- (201) van der Heide, P. *X-Ray Photoelectron Spectroscopy. An Introduction to Principles and Practice*; John Wiley & Sons, Inc.: New Jersey, United States of America, 2012.
- (202) Darkwah, W. K.; Sandrine, M. K. C.; Adormaa, B. B.; Teye, G. K.; Pupilampu, J. B. Solar Light Harvest: Modified d-Block Metals in Photocatalysis. *Catalysis Science and Technology* **2020**, *10*, 5321–5344.
- (203) University of Texas, Chemistry 302. Course material on chemical kinetics. ch302.cm.utexas.edu (accessed April 2015).
- (204) Schulz, M. Polymer derived ceramics in MEMS/NEMS - a review on production processes and application. *Adv. Appl. Ceram.* **2009**, *108*, 454–460.
- (205) del Campo, A.; Arzt, E. Fabrication approaches for generating complex micro- and nanopatterns on polymeric surfaces. *Chem. Rev.* **2008**, *108*, 911–945.
- (206) Ye, C.; Chen, A.; Colombo, P.; Martinez, C. Ceramic microparticles and capsules via microfluidic processing of a preceramic polymer. *J. R. Soc. Interface* **2010**, *7*, 461–473.
- (207) Schulz, M.; Börner, M.; Hausselt, J.; Heldele, R. Polymer derived ceramic microparts from x-ray lithography-cross-linking behavior and process optimization. *J. Eur. Ceram. Soc.* **2005**, *25*, 199–204.
- (208) Eckel, Z. C.; Zhou, C.; Martin, J. H.; Jacobsen, A. J.; Carter, W. B.; Schaedler, T. A.; et al. Additive manufacturing of polymer-derived ceramics. *Science* **2016**, *351*, 58–62.
- (209) Riedel, R.; Mera, G.; Hauser, R.; Kloneczynski, A. Silicon-based polymer-derived ceramics: Synthesis properties and applications-A review. *J. Ceram. Soc. Jpn.* **2006**, *114*, 425–444.
- (210) Riedel, R.; Toma, L.; Fasel, C.; Miehe, G. Polymer-derived mullite-SiC-based nanocomposites. *J. Eur. Ceram. Soc.* **2009**, *29*, 3079–3090.
- (211) Colombo, P.; Mera, G.; Riedel, R.; Sorarù, D.; Riedel, R.; Chen, I.-W. Polymer-derived ceramics: 40 years of research and innovation in advanced ceramics. *Ceram. Sci. Technol.* **2013**, *4*, 245–320.
- (212) Bernardo, E.; Colombo, P.; Pippel, E.; Woltersdorf, J. Novel mullite synthesis based on alumina nanoparticles and a preceramic polymer. *J. Am. Ceram. Soc.* **2006**, *89*, 1577–1583.
- (213) Griggio, F.; Bernardo, E.; Colombo, P.; Messing, G. Kinetic studies of mullite synthesis from alumina nanoparticles and a preceramic polymer. *J. Am. Ceram. Soc.* **2008**, *91*, 2529–2533.
- (214) Baney, R. H.; Chandra, G. In *Encyclopedia of Polymer Science and Engineering*; John Wiley and Sons: New York, 1988; pp 13.
- (215) Pang, Y.; Ijadi-Maghsoodi, S.; Barton, T. J. Catalytic Synthesis of Silylene-Vinylene Preceramic Polymers from Ethynylsilanes. *Macromolecules* **1993**, *26*, 5671–5675.
- (216) Carlsson, D. J.; Cooney, J. D.; Gauthier, S.; Worsfold, J. D. Pyrolysis of Silicon-Backbone Polymers to Silicon Carbide. *J. Am. Ceram. Soc.* **1990**, *73* (2), 237.
- (217) Birot, M.; Pillot, J. P.; Dunogues, J. Comprehensive chemistry of polycarbosilanes, polysilazanes, and polycarbosilazanes as Precursors of Ceramics. *Chem. Rev.* **1995**, *95*, 1443–1477.
- (218) Yajima, S.; Hasegawa, Y.; Okamura, K.; Matsuzawa, T. Development of high tensile strength silicon carbide fibre using an organosilicon polymer precursor. *Nature* **1978**, *273*, 525–527.
- (219) LY, H. Q.; Taylor, R.; Day, R. J.; Heatley, F. Conversion of polycarbosilane (PCS) to SiC based ceramic part I, Characterization of PCS and Curing product. *J. Mater. Sci.* **2001**, *36*, 4037–4043.
- (220) Shimoo, T.; Tsukada, I.; Narisawa, M.; Seguchi, T.; Okamura, K. Change in Properties of Polycarbosilane Derived SiC Fibers at High Temperatures. *J. Ceram. Soc. Jpn.* **1997**, *105* (7), 559–563.
- (221) Bacque, E.; Pillot, J. P.; Birot, M.; Dunogues, J. New polycarbosilane models. 1. Poly[(methylchlorosilylene)methylene], a novel, functional polycarbosilane. *Macromolecules* **1988**, *21*, 30.
- (222) Kim, Y. H.; Shin, D. G.; Kim, H. R.; Park, H. S.; Riu, D. H. Preparation of Polycarbosilane Using a Catalytic Process. *Azo Journal of Materials* **2005**, *287*, 108.
- (223) Hasegawa, Y.; Kobori, T.; Fukuda, K. “Organosilicon Polymer and Process for Production Thereof”. U.S. Pat. No. 4,590,253 (1986).
- (224) Wan, J.; Alizadeh, A.; Taylor, S. T.; Malenfant, P. R. L.; Manoharan, M.; Loureiro, S. M. Nanostructured Non-Oxide Ceramics Templated via Block Copolymer Self-Assembly. *Chem. Mater.* **2005**, *17*, 5613–5617.
- (225) Shi, Y.; Wan, Y.; Zhao, D. Ordered Mesoporous Non-Oxide Materials. *Chem. Soc. Rev.* **2011**, *40*, 3854.
- (226) Chan, V. Z. H.; Hoffman, J.; Lee, V. Y.; Iatrou, H.; Aygeropoulos, A.; Hadjichristidis, N.; Miller, R. D.; Thomas, E. L. Ordered Bicontinuous Nanoporous and Nanorelief Ceramic Films from Self Assembling Polymer Precursors. *Science (Washington, DC, U. S.)* **1999**, *286*, 1716–1719.
- (227) Malenfant, P. R. L.; Wan, J.; Taylor, S. T.; Manoharan, M. Self-Assembly of an Organic – Inorganic Block Copolymer for Nano-Ordered Ceramics. *Nat. Nanotechnol.* **2007**, *2*, 43–46.
- (228) Hoheisel, T. N.; Hur, K.; Wiesner, U. B. Block Copolymer Nanoparticle Hybrid Self-Assembly. *Prog. Polym. Sci.* **2015**, *40*, 3–32.
- (229) Shi, Y. F.; Meng, Y.; Chen, D. H.; Cheng, S. J.; Chen, P.; Yang, H. F.; Wan, Y.; Zhao, D. Y. Highly Ordered Mesoporous Silicon Carbide Ceramics with Large Surface Areas and High Stability. *Adv. Funct. Mater.* **2006**, *16*, 561–567.
- (230) Kamperman, M.; Fierke, M. A.; Garcia, C. B. W.; Wiesner, U. Morphology Control in Block Copolymer/Polymer Derived Ceramic Precursor Nanocomposites. *Macromolecules* **2008**, *41*, 8745–8752.
- (231) Susca, E. M.; Beaucage, P. A.; Hanson, M. A.; Werner Zwanziger, U.; Zwanziger, J. W.; Estroff, L. A.; Wiesner, U. Self-Assembled Gyroidal Mesoporous Polymer-Derived High Temperature Ceramic Monoliths. *Chem. Mater.* **2016**, *28*, 2131–2137.

- (232) Guron, M. M.; Wei, X.; Welna, D.; Krogman, N.; Kim, M. J.; Allcock, H.; Sneddon, L. G. Preceramic Polymer Blends as Precursors for Boron-Carbide/Silicon-Carbide Composites Ceramics and Ceramic Fibers. *Chem. Mater.* **2009**, *21*, 1708–1715.
- (233) Yan, X.-B.; Gottardo, L.; Bernard, S.; Dibandjo, P.; Brioude, A.; Moutaabbid, H.; Miele, P. Ordered Mesoporous Silicoboron Carbonitride Materials via Preceramic Polymer Nanocasting. *Chem. Mater.* **2008**, *20*, 6325–6334.
- (234) Choudhary, A.; Pratihari, S. K.; Agrawal, A. K.; Behera, S. K. Macroporous SiOC Ceramics with Dense Struts by Positive Sponge Replication Technique. *Adv. Eng. Mater.* **2018**, *20*, 1700586.
- (235) Han, L.; Song, S.; Liu, M.; Yao, S.; Liang, Z.; Cheng, H.; Ren, Z.; Liu, W.; Lin, R.; Qi, G.; Liu, X.; Wu, Q.; Luo, J.; Xin, H. L. Stable and efficient single-atom Zn catalyst for CO₂ reduction to CH₄. *J. Am. Chem. Soc.* **2020**, *142*, 12563–12567.
- (236) Zhu, D. D.; Liu, J. L.; Qiao, S. Z. Recent advances in inorganic heterogeneous electrocatalysts for reduction of carbon dioxide. *Adv. Mater.* **2016**, *28* (18), 3423–3452.
- (237) Liu, X.; Yang, H.; He, J.; Liu, H.; Song, L.; Li, L.; Luo, J. Highly active, durable ultrathin MoTe₂ layers for the electroreduction of CO₂ to CH₄. *Small* **2018**, *14* (16), No. 1704049.
- (238) Kuhl, K. P.; Hatsukade, T.; Cave, E. R.; Abram, D. N.; Kibsgaard, J.; Jaramillo, T. F. Electrocatalytic conversion of carbon dioxide to methane and methanol on transition metal surfaces. *J. Am. Chem. Soc.* **2014**, *136* (40), 14107–14113.
- (239) Shen, J.; Kortlever, R.; Kas, R.; Birdja, Y. Y.; Diaz-Morales, O.; Kwon, Y.; Ledezma-Yanez, L.; Schouten, K. J. P.; Mul, G.; Koper, M. T. M. Electrocatalytic reduction of carbon dioxide to carbon monoxide and methane at an immobilized cobalt protoporphyrin. *Nat. Commun.* **2015**, *6*, 8177.
- (240) Li, W.; Herkt, B.; Seredych, M.; Bandoz, T. J. Pyridinic-N groups and ultramicropore nanoreactors enhance CO₂ electrochemical reduction on porous carbon catalysts. *Appl. Catal., B* **2017**, *207*, 195–206.
- (241) Manthiram, K.; Beberwyck, B. J.; Alivisatos, A. P. Enhanced electrochemical methanation of carbon dioxide with a dispersible nanoscale copper catalyst. *J. Am. Chem. Soc.* **2014**, *136* (38), 13319–13325.
- (242) Zhao, Z.; Peng, X.; Liu, X.; Sun, X.; Shi, J.; Han, L.; Li, G.; Luo, J. Efficient and stable electroreduction of CO₂ to CH₄ on CuS nanosheet arrays. *J. Mater. Chem. A* **2017**, *5* (38), 20239–20243.
- (243) Li, M.; Wang, H.; Luo, W.; Sherrell, P. C.; Chen, J.; Yang, J. Heterogeneous Single-Atom Catalysts for Electrochemical CO₂ Reduction Reaction. *Adv. Mater.* **2020**, *32*, 2001848.
- (244) Sheng, T.; Sun, S.-G. Free energy landscape of electrocatalytic CO₂ reduction to CO on aqueous FeN₄ center embedded graphene studied by ab initio molecular dynamics simulations. *Chem. Phys. Lett.* **2017**, *688*, 37.
- (245) Wang, X.; Chen, Z.; Zhao, X.; Yao, T.; Chen, W.; You, R.; Zhao, C.; Wu, G.; Wang, J.; Huang, W.; Yang, J.; Hong, X.; Wei, S.; Wu, Y.; Li, Y. Regulation of Coordination Number over Single Co Sites: Triggering the Efficient Electroreduction of CO. *Angew. Chem., Int. Ed.* **2018**, *57*, 1944.
- (246) Lu, F.; Bao, H.; Mi, Y.; Liu, Y.; Sun, J.; Peng, X.; Qiu, Y.; Zhuo, L.; Liu, X.; Luo, J. Electrochemical CO₂ reduction: from nanoclusters to single atom catalysts. *Sustainable Energy Fuels* **2020**, *4*, 1012.
- (247) Mistry, H.; Reske, R.; Zeng, Z. H.; Zhao, Z. J.; Greeley, J.; Strasser, P.; Cuenya, B. R. highly selective plasma-activated copper catalysts for carbon dioxide reduction to ethylene. *Nat. Commun.* **2014**, *136*, 16473–16476.
- (248) Russier-Antoine, I.; Bertorelle, F.; Vojkovic, M.; Rayane, D.; Salmon, E.; Jonin, C.; Dugourd, P.; Antoine, R.; Brevet, P.-F. on-linear optical properties of gold quantum clusters. The smaller the better. *Nanoscale* **2014**, *6*, 13572–13578.
- (249) Wang, L.; Chen, W.; Zhang, D.; Du, Y.; Amal, R.; Qiao, S.; Wu, J.; Yin, Z. Surface strategies for catalytic CO₂ reduction: from two-dimensional materials to nanoclusters to single atoms. *Chem. Soc. Rev.* **2019**, *48*, 5310–5349.
- (250) Raton, B. et al. *The Science of Miniaturization*, 2nd ed.; CRC Press.
- (251) Aires, F. J. C. S.; et al. Pd catalysts supported on silicon nitride for the combustion of methane: Influence of the crystalline and amorphous phases of the support and of the preparation method on the catalytic performances. *Catal. Today* **2006**, *117*, 518–524.
- (252) Loricera, C. V.; Alvarez-Galvan, M. C.; Guil-Lopez, R.; Ismail, A. A.; Al-Sayari, S. A.; Fierro, J. L. G. Structure and reactivity of sol-gel V/SiO₂ catalysts for the direct conversion of methane to formaldehyde. *Top Catal* **2017**, *60*, 1129–1139.
- (253) Landry, C. J.T.; Coltrain, B. K.; Wesson, J. A.; Zumbulyadis, N.; Lippert, J. L. In situ polymerization of tetraethoxysilane in polymers: chemical nature of the interactions. *POLYMER* **1992**, *33* (7), 1496–1506.
- (254) Glassman, I.; Yetter, R. A.; Glumac, N. *Combustion*; Elsevier, 2014.
- (255) Rogers, W. J. The effects of sterilization on medical materials and welded devices. *Join. Assem. Med. Mater. Devices* **2013**, 79–130.
- (256) Stivala, S. S.; Reich, L. Structure vs stability in polymer degradation. *Polym. Eng. Sci.* **1980**, *20* (10), 654–661.
- (257) Chen, F.; Qian, J. Studies on the thermal degradation of polybutadiene. *Fuel Process. Technol.* **2000**, *67* (1), 53–60.
- (258) Ray, S.; Cooney, R. P. Thermal Degradation of Polymer and Polymer Composites. *Handb. Environ. Degrad. Mater.* **2012**, 213–242.
- (259) Wei, X.; Luo, T. Chain length effect on thermal transport in amorphous polymers and a structure–thermal conductivity relation. *Phys. Chem. Chem. Phys.* **2019**, *21* (28), 15523–15530.
- (260) Singh, G.; Esmaeilpour, M.; Ratner, A. Effect of polymeric additives on ignition, combustion and flame characteristics and soot deposits of crude oil droplets. *Combust. Sci. Technol.* **2023**, 195, 1299.
- (261) de Almeida Silva, M.; Romagnoli, E. S.; Carvalho Pereira, R. d.; Tarley, C. R. T.; Segatelli, M. G. Structure and porosity of silicon oxycarbide/carbon black composites. *Mater. Chem. Phys.* **2020**, *254*, No. 123503.
- (262) Cai, L.; Luo, J.; Wang, M.; Guo, J.; Duan, J.; Li, J.; Li, S.; Liu, L.; Ren, D. Pathways for municipalities to achieve carbon emission peak and carbon neutrality: A study based on the LEAP model. *Energy* **2023**, *262*, 125435.
- (263) Tan, Z. H.; Kong, X. Y.; Ng, B.-J.; Soo, H. S.; Mohamed, A. R.; Chai, S.-P. Recent advances in defect-engineered transition metal dichalcogenides for enhanced electrocatalytic hydrogen evolution: perfecting imperfections. *ACS Omega* **2023**, *8*, 1851–1863.
- (264) Liu, H.; Chen, K.; Feng, Y.-N.; Zhuang, Z.; Chen, F.-F.; Yu, Y. In Situ confined growth of Co₃O₄-TiO₂/C S-scheme nanoparticle heterojunction for boosted photocatalytic CO₂ reduction. *J. Phys. Chem. C* **2023**, *127*, 5289–5298.
- (265) Rodriguez Herrero, Y.; Ullah, A. Hydrophobic polyhedral oligomeric silsesquioxane support enhanced methanol production from CO₂ hydrogenation. *ACS. Appl. Mater. Interfaces* **2023**, *15*, 14399–14414.
- (266) Dey, S.; Manjunath, K.; Zak, A.; Singh, G. WS₂ nanotube-embedded SiOC fiber mat electrodes for sodium-ion batteries. *ACS Omega* **2023**, *8*, 10126–10138.
- (267) Okoroanyanwu, U.; Bhardwaj, A.; Watkins, J. J. Large area millisecond preparation of high-quality, few-layer graphene films on arbitrary substrates via Xenon flash lamp photothermal pyrolysis and their application for high-performance micro-supercapacitors. *ACS. Appl. Mater. interfaces* **2023**, *15*, 13495–13507.
- (268) United Nations Development Program. Preceramic polymers grafted to SiO₂ nanoparticles via metal coordination pyrolyzing with high ceramic yields: Implications for aerospace propulsion and biomedical coatings. *ACS. Appl. Nano Mater.* **2023**, *6*, 3661–3674.
- (269) Wang, H.; Li, X.; Jiang, Y.; Li, M.; Xiao, Q.; Zhao, T.; Yang, S.; Qi, C.; Qiu, P.; Yang, J.; Jiang, Z.; Luo, W. A universal single-atom coating strategy based on tannic acid chemistry for multifunctional heterogeneous catalysis. *Angew. Chem.* **2022**, *134*, 202200465.
- (270) Srivastava, R. K.; Sarangi, P. K.; Bhatia, L.; Singh, A. K.; Shadangi, K. P. Conversion of methane to methanol: technologies and future challenges. *Biomass Conv. & Bioref.* **2022**, *12*, 1851–1875.

(271) Tanimu, A.; Tanimu, G.; Ganiyu, S. A.; Gambo, Y.; Alasiri, H.; Alhooshani, K. Metal-free catalytic oxidative desulphurization of fuels – A review. *Energy Fuels* **2022**, *36*, 3394–3419.